Title
Computer Simulation of Breast Cancer Screening

Author
Halat, Nilram

Publication Date
2023

Peer reviewed|Thesis/dissertation

Computer Simulation of Breast Cancer Screening

By

NILRAM HALAT

THESIS

Submitted in partial satisfaction of the requirements for the degree of

MASTER OF SCIENCE

in

Biomedical Engineering

in the

OFFICE OF GRADUATE STUDIES

of the

UNIVERSITY OF CALIFORNIA

DAVIS

Approved:

_____

John M. Boone, Chair

_____

J. Anthony Seibert

_____

Ramsey D. Badawi

Committee in Charge

2023

Abstract

The purpose of this project was to enhance breast cancer screening by identifying the factors that impact it. Breast cancer is the most common cancer diagnosed in women, and American women have a 12.3% risk of contracting it at some point in their life. Although screening has proven to be successful, controversies surrounding breast cancer screening programs remain. The screening start age, end age and frequency are subjects of the debate. This project aimed to address these controversies by developing a computer simulation of breast cancer screening. The simulation used rejection sampling to generate a cohort of 1 million women with 5 main attributes which are 1) age in the year 2016, 2) race, 3) age of death from non-breast cancer causes, 4) age at which the breast cancer was contracted, and 5) the growth rate of breast cancer. We then examined the generated cohort with different screening procedures. The study focused on mammography and breast CT screening modalities. To determine the most efficient breast cancer screening protocol several parameters were of interest. One of these parameters was years of life saved per number of tests performed. We concluded that screening every 2 years with CT starting at age 50 until 80 has the highest years of life saved per number of screenings for the entire population. The study also suggests that races benefit differently from each screening program, which should be taken into account for screening policies.

1. Introduction

In the United States (US), one in every eight women will develop breast cancer at some point in her lifetime. This translates to approximately a 12.3% lifetime risk of developing breast cancer [1, 2]. Approximately 316120 new cases of breast cancer were diagnosed among US women in 2017, and an estimated 40610 women in the country were expected to die from breast cancer in that year. In the US alone there were more than 3.5 million women with a history of breast cancer who were alive at the beginning of the year 2016 [3, 4]. Breast cancer accounts for more than 1 in 10 new cancer diagnoses every year, making it the most common cancer diagnosed in women. After lung cancer, breast cancer is the leading cause of cancer death among women. [5-7]

An assessment of breast cancer demographics from the year 2010 to 2014 has shown the median age of breast cancer diagnosis to be 62 years old [8]. In general, breast cancer incidence and mortality increase with age. Factors such as ethnic background and socioeconomic status also affect breast cancer mortality and incidence. For instance, in the US, death rates from breast cancer are higher for black women than white women while incidence rates are higher for white women than black women [9, 10]. Black women are found to have 59 as their median age of breast cancer diagnosis, while that of white women is 63 years old [8].

Screening is used to find cancer when it is still small and curable, which results in a reduction of breast cancer mortality [11]. The evidence that mammography leads to reduced death rates is provided by randomized controlled trials (RCTs) [12-14]. One of the most recent RCTs in screening mammography started in 1982 in Gothenburg, Sweden. A random sample of around 52000 women aged 39 to 59 was selected and was offered 2-view mammography screening every 18 months [15]. The women invited for screening experienced a reduction of 23% in mortality after a follow-up period of 14 years [16].

Different screening modalities are used for breast cancer detection. Among them are mammography, MRI, Ultrasound, and Computerized Tomography (CT). These modalities are constantly being studied to assess their effectiveness in breast cancer screening. Breast cancer screening leads to earlier detection of breast cancer. As treatment is more effective in earlier stages of the disease, early detection results in a better prognosis and lower mortality rates.

Since the adoption of screening mammography in the US in the 1980s, there has been a steady decrease in women's age-adjusted breast cancer mortality [11]. In current practice, mammography has the highest sensitivity to identify breast cancer at an earlier phase [17]. Despite the proven success of screening, and mammography in particular, there are controversies regarding breast cancer screening programs. Approximately a third of women above age 40 do not receive screening regularly in the US. The low compliance may be due to the lack of a national consensus on the screening guidelines [11]. It should be acknowledged that these controversies stem from factors which go beyond science. For instance, differing perceptions of epidemiological data, financial competition between insurance payers and radiologists, and politics of advocacy-driven research stimulate these controversies.

One aspect of the controversy is whether women should start screening at age 40 or 50, and how often they should undergo screening. Furthermore, the age at which screening should be conducted is also debatable. Another question is whether people with different risk factors, for instance, depending on their race, should be screened with a different program.

The three main organizations that have issued guidelines for breast cancer screening in the US are the US Preventive Services Task Force (USPSTF), the American Cancer Society (ACS), and the American College of Radiology (ACR). The consensus among the three organizations is that screening mammography saves lives and should be performed in women aged 50-74 [11]. However, while panels have been held to resolve the debatable issues, they have not resulted in a consensus on the screening program to be conducted. For instance, the USPTF recommends screening women aged 50 to 74 biennially using mammography while the ACS recommends women aged 50 to 54 to be screened with mammography annually, and women older than 55 to have the choice of continuing screening annually or transitioning to biennial screening. Furthermore, the USPTF suggests a personal choice of biennial screening with mammography for women prior to age 50. On the other hand, according to the ACS, women aged 40 to 44 should have the choice to undergo annual screening mammography while women aged 45 to 49 should be screened with mammography annually [14, 18-20]. The ACR recommends annual screening with mammography for women aged 40 to 74 [21, 22].

We developed a computer simulation of breast cancer screening in this research project to address the issues and controversies mentioned above. A set of selected parameters which influence breast cancer screening was modeled in the simulation. The influence of each of these parameters on the simulated breast cancer outcome was evaluated by slightly changing the parameters.

We developed a database which characterizes the female population in the United States. The database reflects appropriate age and racial distributions along with death rates from non-breast cancer causes and breast cancer incidence. We developed a cohort simulator with the capability of generating a cohort of women in which 5 main attributes were assigned to each female within the cohort. The attributes are 1) age in the year 2016, 2) race, 3) age of death from non-breast cancer causes, 4) age at which the breast cancer was contracted, and 5) the growth rate of breast cancer. Different screening procedures were examined on the aforementioned database. The screening modalities studied were mammography and breast CT. Several parameters of interest were studied on the results of the different screening procedures to determine the most efficient breast cancer screening protocol.

The goal of our research project was to gain a better understanding of the factors that affect breast cancer screening, and to use that knowledge for improving breast cancer screening techniques.

It should be noted that while this study focuses on masses, not all breast cancers are in the form of a distinct mass or tumor. An example of tumor-free cancers is inflammatory breast cancer (IBC). Symptoms of this cancer may be inflammation of the breast or distortions in the breast skin. IBC is often wrongly diagnosed as mastitis or an infection. Detection of IBC relies heavily on biopsy and includes physical examination, patient history, and pathology results. [23, 24]

As mentioned, targeting masses is one of several breast cancer endpoints, and focusing on masses and using solid tumor size as the only indicator of breast cancer pose a limit to the findings of this study.

2. Methods

In this chapter, the general methods used throughout the project are explained. The importance of simulation methods in various sciences has significantly grown in the past several years. These methods are an integral part of computational sciences such as computational physics and computational chemistry. Computation has been recognized as a third approach for advancing the natural sciences along with theory and traditional experimentation. This recognition is due to the growing power of computers and advances in simulation methodology. Random number generation is at the heart of simulation and many standard statistical methods [25].

2.1 Random Number Generation

A sequence of numbers is considered random if the next number cannot be predicted from the previous one. [26, 27] Concepts such as probability space and random variables are the basis for the fields of probability and statistics. [28]

The need for producing unpredictable results has led to the development of a process called random number generation. In this process, a random number generator (RNG) produces a sequence of numbers or symbols that cannot be predicted by reason and depend on random chance. Computer simulations and statistical sampling are among the applications of random number generation.

Two types of RNGs exist depending on the method by which they generate the random numbers. The first type leads to the generation of "True" random numbers by measuring some physical phenomenon expected to occur at random and then offsetting any measurement biases. Examples of "True" RNGs are measuring radioactivity or thermal noise. A drawback of True RNGs is that the sequence of numbers cannot be reproduced which renders verification of the calculation methods difficult. [29]

The second type of RNGs utilizes computational algorithms which can produce long sequences of random results. These sequences only appear random but are fully determined by a shorter initial value called a seed. Consequently, with a known seed value the apparently random sequence can be reproduced in its entirety. These types of RNGs are called pseudorandom number generators (PRNGs). PRNGs are not typically reliant on sources of natural phenomena which allows them to not be limited by an external event. While PRNGs do not generate truly random sequences they are practical because of their reproducibility and speed in random number generation. These properties make PRNGs central in applications such as simulations.

Deterministic algorithms generate pseudorandom numbers. Pseudorandom numbers are considered random because they pass statistical tests relevant to their distribution and correlation. MATLAB® RNGs are algorithms that are used to generate pseudorandom numbers with a prescribed distribution. Methods that generate pseudorandom numbers differ in the distribution used to produce the numbers. For instance, the rand function in MATLAB® returns random numbers from a uniform distribution. Three common pseudorandom number generation methods include the direct method, the inversion method, and the accept-reject

(rejection sampling) method. These methods can be used to generate random numbers from different distributions. [30]

Random number generation was used in this study to perform statistical sampling and computer simulation. Utilizing MATLAB® for conducting the simulations, built-in MATLAB® RNGs were used to develop the randomness required in generating our data. The randomness was controlled by a process called rejection sampling for the simulations to accurately reflect the statistical data used in our samplings. Rejection sampling is explained in the next section.

2.2 Rejection Sampling

Rejection sampling is a method for generating random samples from a distribution that is difficult to sample from directly. The basic idea behind rejection sampling is to sample from a distribution that is easy to sample from, called the proposal distribution, and then accept or reject the sample based on its likelihood under the target distribution.

To perform rejection sampling, we first need to define the target distribution and the proposal distribution. The target distribution represents the distribution that we are interested in sampling from, while the proposal distribution is a distribution that we can easily sample from. The proposal function should encapsulate the target function. In other words, if the probability density function (PDF) of the target distribution is $p(x)$ and the PDF of the proposal distribution is $q(x)$ there needs to be a constant k where $k \times q(x) \geq p(x)$ for all x.

Next, we need to determine an acceptance criterion or a value for the acceptance threshold. This value determines the probability of accepting a sample from the proposal distribution. The acceptance threshold is typically set based on the ratio of the PDFs of the target and proposal distributions. In our case specifically, the acceptance threshold is set to $p(x)/(k \times q(x))$.

Once we have defined the target and proposal distributions and determined the acceptance threshold, we can generate samples from the proposal distribution and accept or reject them based on the acceptance threshold. To do this, we generate a sample x from the proposal distribution and then generate a random number u between 0 and 1 from the uniform distribution $U(0,1)$. If u is less than the acceptance threshold, we accept sample x, otherwise, we reject it and repeat the process.

Figure 2.2.1 (a,b,c) illustrates an example of rejection sampling. $p(x)$ and $q(x)$ are the target and proposal density functions respectively. Figure 2.2.1-b indicates the target and scaled proposal function. Figure 2.2.1-c shows the normalized histogram of the samples generated using rejection sampling.

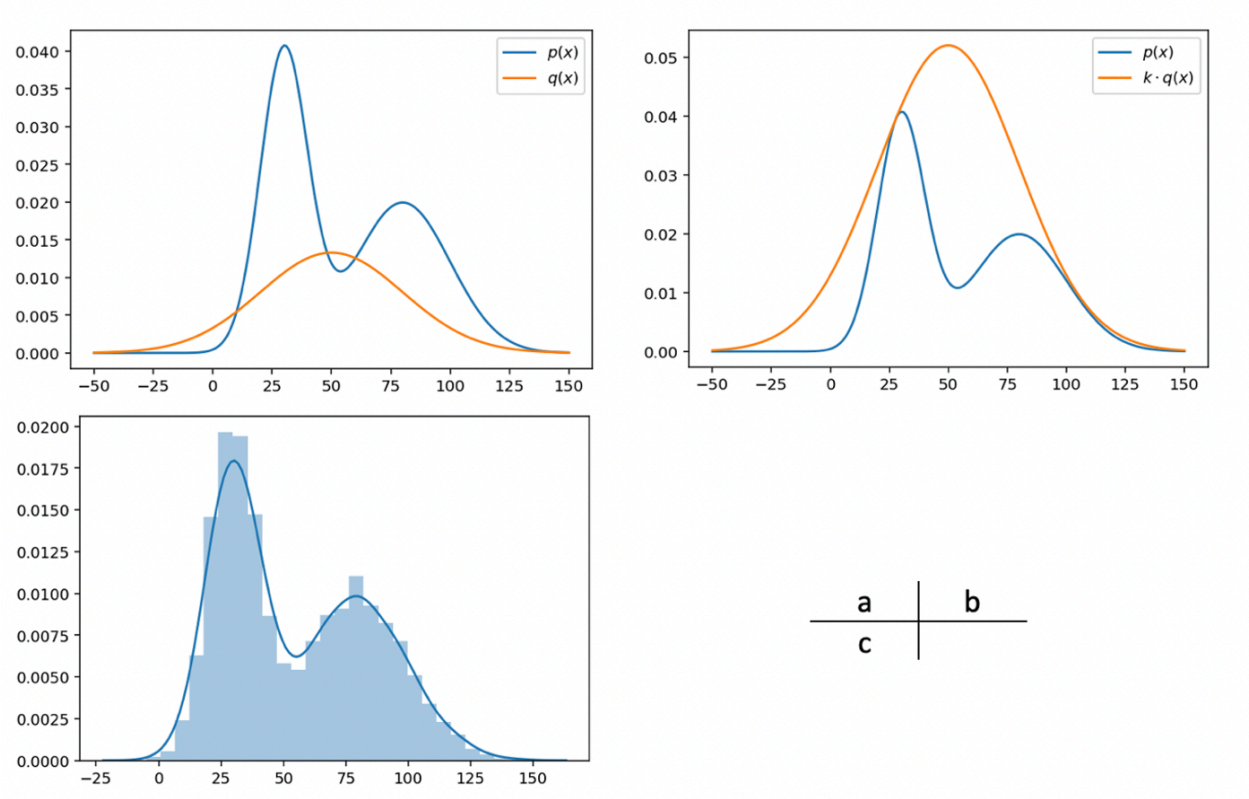

Fig 2.2.1 Rejection Sampling Performance Example

An example of a proposal distribution that can be used for all target distributions in rejection sampling is the uniform distribution where k is $max(f(x))$. While this proposal distribution works for all target distributions, it is not the most efficient proposal distribution as there may be a relatively large number of rejected samples. The proposal distribution chosen should be as close to the target distribution as possible while maintaining the requirements of an acceptable proposal distribution.

Overall, while rejection sampling is a useful technique for generating random samples from complex distributions, it has its limitations. One of the key benefits of rejection sampling is that it can be used to generate samples from a wide range of distributions, as long as we can define a suitable proposal distribution. On the other hand, the acceptance rate or the proportion of samples that are accepted may be quite low, especially for distributions with highly skewed or multi-modal shapes. This can make rejection sampling computationally expensive, as it may require a large number of samples to be generated in order to obtain a sufficient number of accepted samples.

This project consisted of multiple sections, each of which included simulations of statistical data. Rejection sampling was the method used to accurately sample the statistical data to be simulated.

2.3 Microsimulation

Microsimulation is a type of computer modeling that captures a highly detailed analysis of activities. Activities such as spread of disease by pathogens, financial transactions, or flow of highway traffic can accurately be modeled with microsimulation. The difference between microsimulation and other modeling techniques is in considering the interaction of individual ("micro") units such as people, vehicles, households, or businesses. Microsimulation treats each unit as an individual and autonomous entity. It leverages stochastic parameters to take into account individual tendencies and preferences. For instance, in the model for spread of disease, contributing factors such as resistance to the virus and personal habits such as hygiene vary among individuals and should be taken into account. Similarly, in the highway traffic model, driver preferences such as cautiousness or aggressiveness affect their driving and need to be considered [31].

Microsimulation is usually used to study the influence of some proposed changes or interventions such as government policies before they can be implemented in the real world. These models were developed as a guide for US social policy decisions in the 1970s [32]. Microsimulation is especially useful when carrying out tests on hypotheses is difficult or not practical to implement in the real world; for example, when such tests take long years to gather the needed information and determine the implications of the changes. Microsimulation provides a relatively cost-efficient method to inform policy changes and decisions [33].

According to the International Microsimulation Association, microsimulation is a modeling approach that functions at the level of individual units. The model denotes each unit by a record that includes a unique identifier and a set of parameters or attributes associated with the unit. An example of records is a list of people with known age, gender, employment, and marital status. Another example is a list of vehicles with a known model, origin, and destination. Units are described using a series of deterministic or stochastic rules which lead to simulated changes in behavior and state. Chances of dying, marrying, giving birth, or moving are examples of stochastic rules while changes in tax liability that result from changes in tax rules are an example of a deterministic rule. The estimated outcome of these rules determines the results [34].

One of the main uses of microsimulation is in the health sciences. The application of microsimulation in health policy decisions dates back to 1985 when "Microsimulation Screening Analysis" (MISCAN) was developed by Habbema and colleagues [35]. MISCAN models were used to evaluate the impact of screening on breast, prostate, colorectal and cervical cancer [36-39]. Some examples of applications of microsimulation in health sciences include transmission of infectious diseases such as smallpox, influenza, and HIV [40-45]. As described earlier, microsimulation can generate individuals independent of each other to simulate life histories. These life histories can be aggregated to estimate the comparative efficacy of treatments and prevention strategies at the population level. Microsimulation can be used for health policy decisions by generating predictions such as prediction of death rates and disease incidence trends of different policies [46, 47].

An example of microsimulation for breast cancer is the OncoSim-Breast, a Canadian simulation model. In this simulation model, developed to study breast cancer interventions, the start, growth, and spread of tumors were simulated. The combination of breast cancer incidence, death rates, and cost of the screening program was used to project the screening outcomes in the population. The simulation allowed for different inputs from users to compare outcomes and answer questions. The result of this project was a close projection of observed data in Canada, and observations in the UK. In conclusion, the reproducibility of the outcomes rendered this microsimulation usable to inform policies regarding early breast cancer detection. [48]

A practically similar approach was taken in our microsimulation project for breast cancer in the US. We used US female population data on age, race, mortality, and breast cancer incidence along with breast cancer growth rates to develop a cohort of women reflecting the population. Then, screening programs differing in screening start and end age, and screening frequency were applied to the cohort created to determine the efficacy of each program. This simulation was a microsimulation because the study was conducted on a micro level and the life histories of each person were developed and studied for the research to reach a conclusion. The simulated life histories were aggregated to estimate population-level results. In the end, the population-level results helped determine the most efficient breast cancer screening program.

Throughout this project, random number generators and rejection sampling were implemented to develop the simulations using MATLAB® software.

3 The Cohort Generation Model

In this chapter, the steps taken to generate the cohort of women studied in the project are explained.

3.1 Demographics Model

Demographics Database

A database was developed to characterize the female population in the United States. The database was designed to reflect appropriate age and racial distributions. High-resolution (1-year interval) population statistics were downloaded from the US Census Bureau website [49] and are shown in figure 3.1.1. As seen in the figure, data was available for five races; White, Black or African American, American Indian or Alaska Native, Asian, Native Hawaiian, and Other Pacific Islander. The plots show the number of women residing in the US by age for each race.

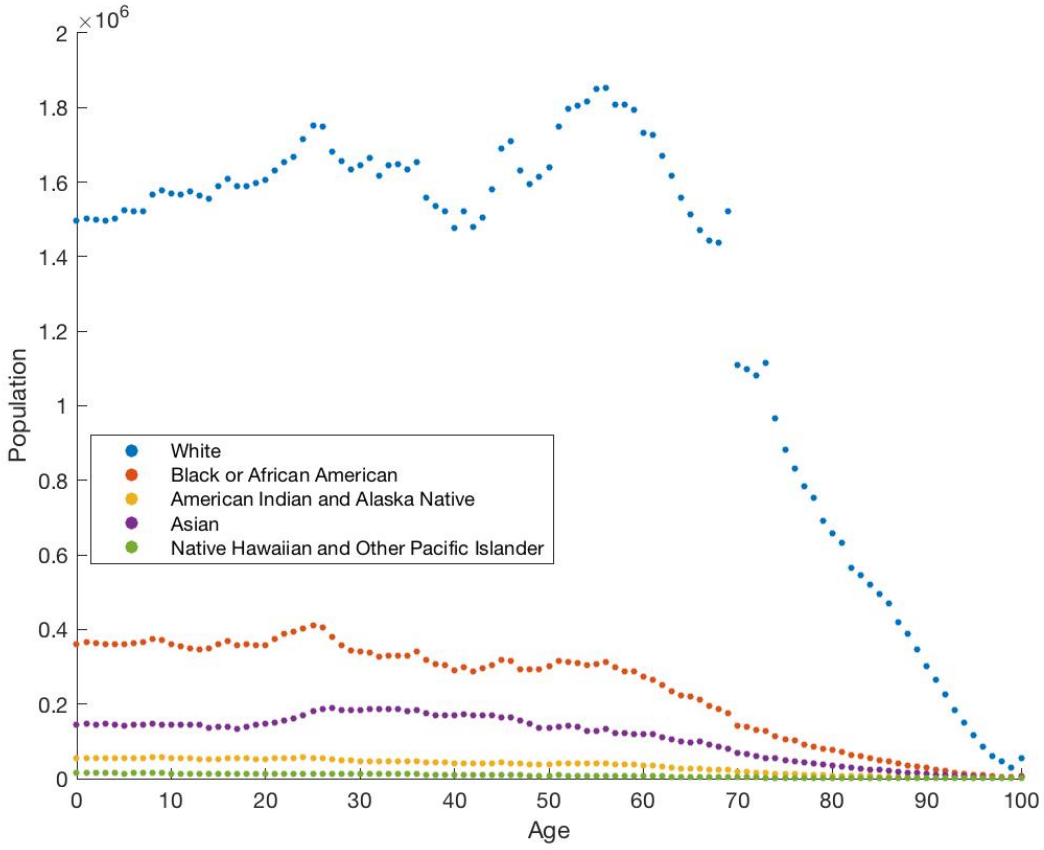

Fig 3.1.1 US Female Population by Age and Race on July 1, 2016

The data shown in Figure 3.1.1 includes individuals who might have reported more than a single race when surveyed. Consequently, summing the data from the five races shown in Figure 3.1.1 results in a number larger than the actual total population.

Population Model Methods

Data for total (all races combined) was also available on the US Census website but at the lower resolution of 5-year intervals. [50] The ratio of the actual total population (5-year total) to the sum of the five races (Total B) was 0.97186. This ratio was used to compute the more accurate high-resolution data for total (Total A). The ratio was also used to scale the data for each of the five races so that the sum of all five races would result in the accurate total population. Illustrated in figure 3.1.2 are the high resolution 1-year interval total by summation shown in the red line, the five-year interval actual total shown by bullet symbols and the recomputed high-resolution total shown by the dotted line.

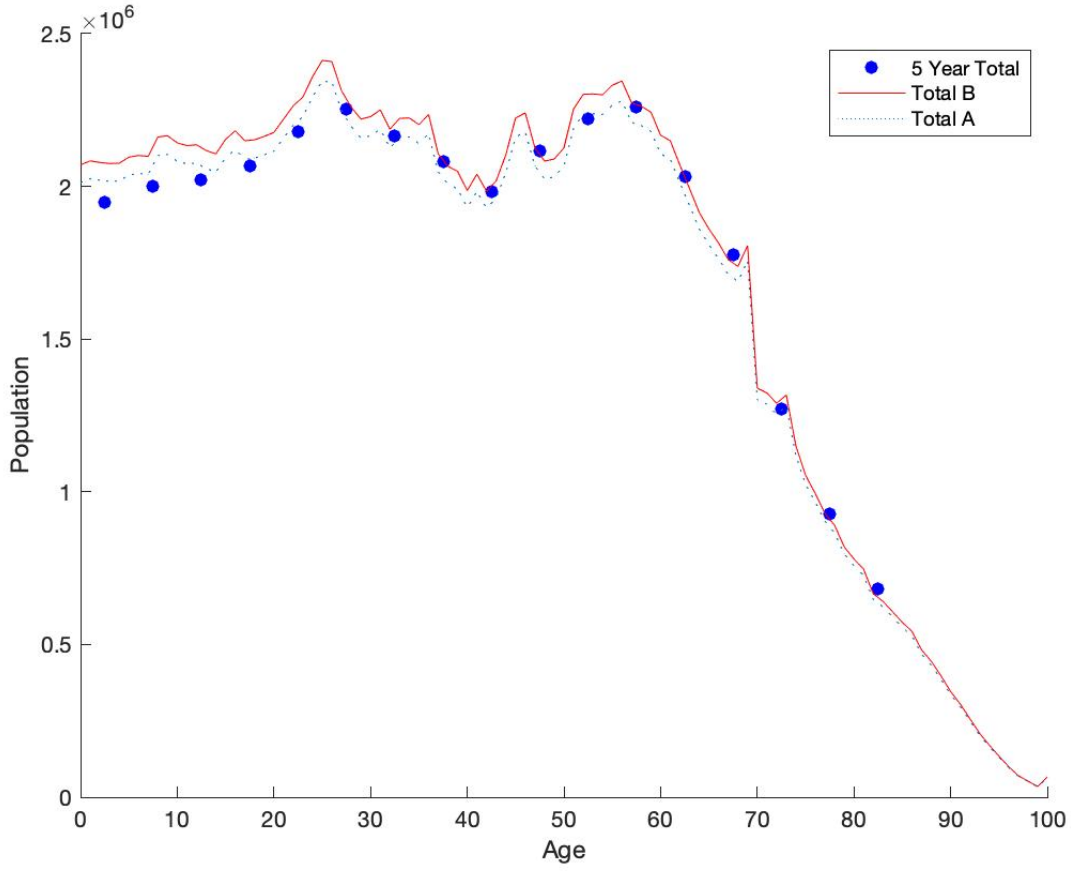

Fig 3.1.2 Total (All Races Combined) Population by Age

The data was then validated for consistency after the rescaling. For instance, we made sure that the new total equals the sum of the five races after they were multiplied by the

scaling factor separately. The results matched as expected.

The resulting datasets (five races and total) were modeled using the accept-reject method explained in section 2.2. to assign appropriate ages and races to the 10^6 simulated women in our generated cohort. This assigned age denotes the age of each woman on July 1, 2016. A numerical flag was also assigned to characterize each person's racial background.

Model Results

The results from the model for 10^6 simulated women are shown in figure 3.1.4. The model results are plotted along with the matching raw data which verifies the model. The bullets show the raw data, and the dotted lines are the results from the model.

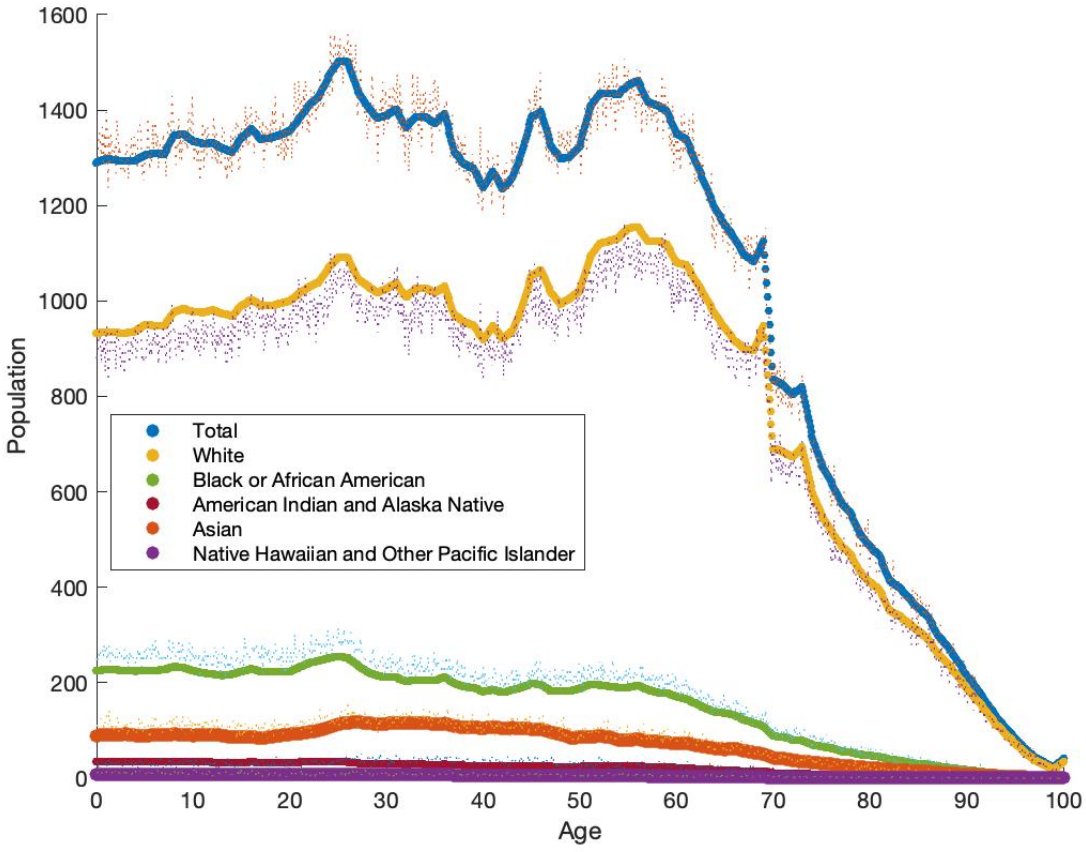

Fig 3.1.4 Demographics Model Results and Raw Data

Five different cohorts of women were generated and saved to our database for further study. The different cohorts were obtained by changing the seed for the random number generator used in the simulations. The results were compared and are shown for the

total (all races combined) in figure 3.1.5. The solid symbols illustrate the mean population at each age and the error bars represent ±1 standard deviation (SD).

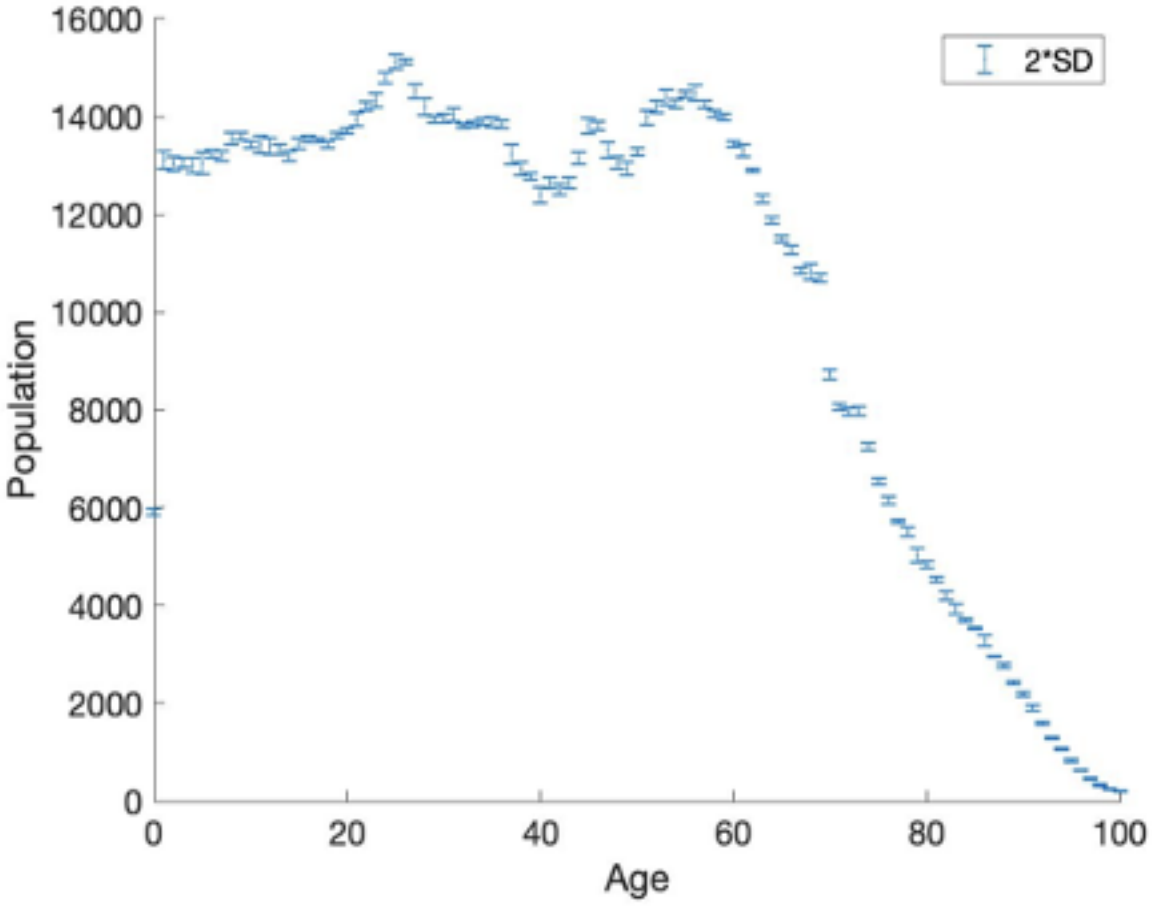

Fig 3.1.5 Comparison of Five Generated Cohorts for Total (All Races Combined)

3.2 Death Model

Death Rates Data

Because the prognosis model (as will be discussed in chapter 4) deals with the probability of dying from breast cancer independently from other causes of death, death rates due to all causes except breast cancer were sought for the general population.

The objective was to obtain the age at which each woman in our cohort would die from all causes other than breast cancer. The Center for Disease Control and Prevention (CDC) website [51] had five-year resolution death rates from all causes, but not from all causes excluding breast cancer.

This data, shown in figure 3.2.1 includes rates of death from all causes in the US female population for all races combined, and the four races of White, Black, American Indian or Alaska Native, and Asian or Pacific Islander. The rates are per 100,000 population in each specified group. While the general range of the age groups is 5 years, people 85 and above are categorized as one age group. According to the source of the data, it is important to note that because of inconsistencies in censuses, surveys, and death certificate race reportings one should take caution when interpreting the data for races other than White and Black.

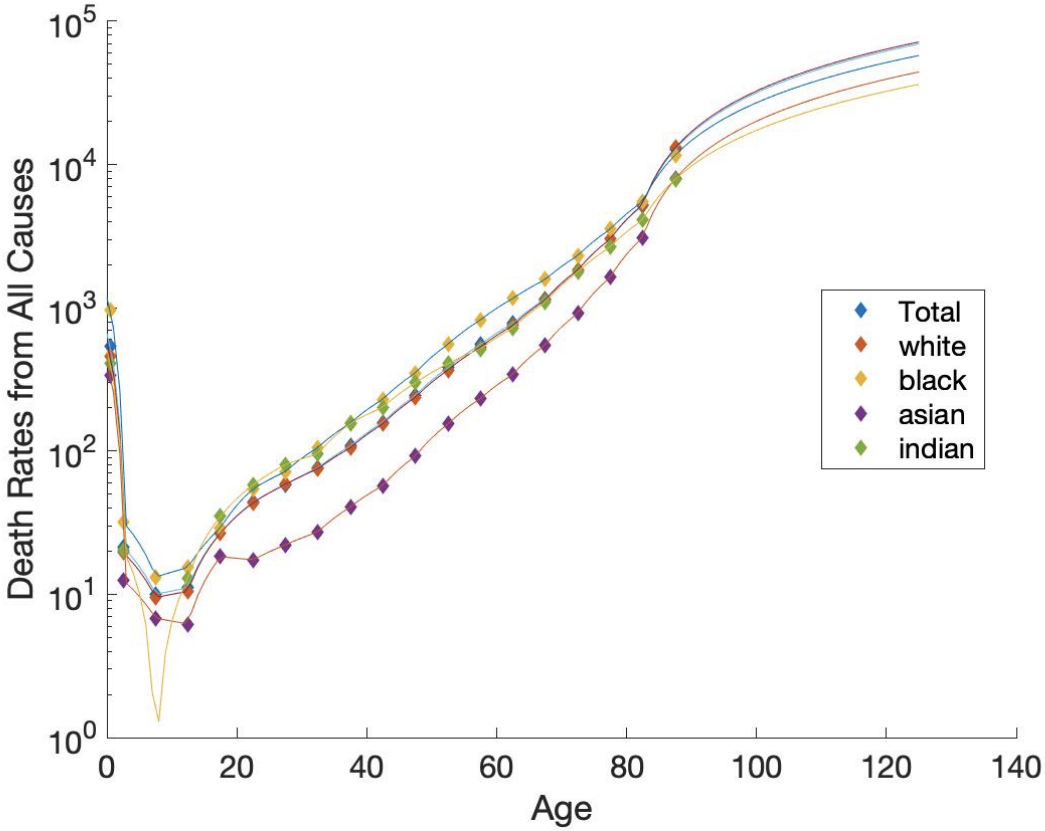

Fig 3.2.1 US Female Death Rates per 100,000 from All Causes by Age and Race

Data for mortality rates by age from breast cancer were available on the Surveillance, Epidemiology, and End Results Program (SEER) website [52]. This data, shown in figure 3.2.2 includes death rates from breast cancer for the US female population for all races combined and the four races of White, Black, American Indian or Alaska Native, and Asian or Pacific Islander. Hispanics and Non-Hispanics are not mutually exclusive from whites, blacks, Asian/Pacific Islanders, and American Indians or Alaska Natives. The rates are per 100,000 and are at a 5-year resolution. People 85 and older are categorized as one age group.

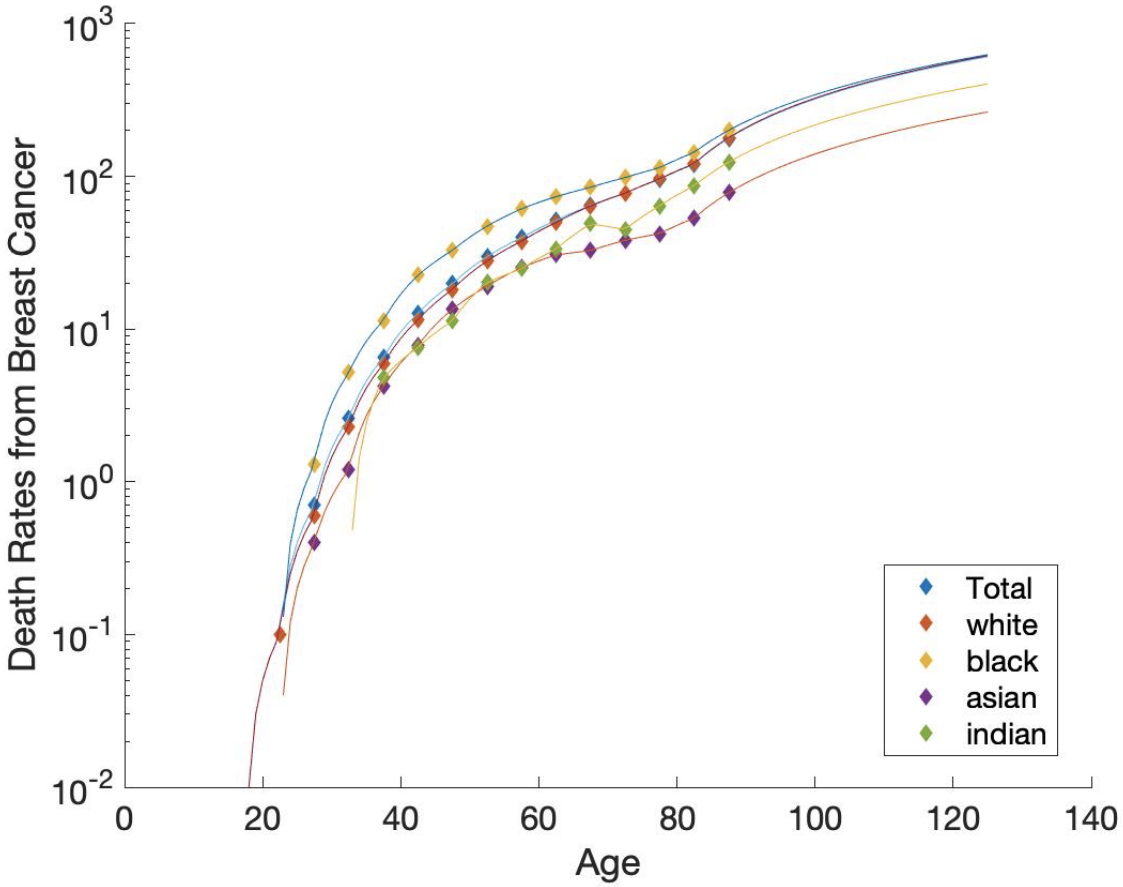

Fig 3.2.2 US Female Death Rates per 100,000 Population from Breast Cancer by Age and Race

Death Model Methods

As mentioned earlier, we aimed to determine the ages of death from any cause other than breast cancer for the normal US population. Mortality rates due to breast cancer were subtracted from death rates from all causes in order to obtain rates of death from all causes except breast cancer.

The data for both death rates from all causes and death rates from breast cancer categorizes people 85 and above into a single group. Based on the list of verified oldest people, the oldest woman in the world has lived up to age 123. Thus, a data point illustrating

a 100% probability of dying at age 125 was added to the data in order to obtain more accuracy at older ages. Figure 3.2.3 illustrates the resulting death rates at 5-year intervals and the corresponding interpolations to 1-year interval resolution.

While the data for population by age and race were available for total and the five racial categories of White, Black or African American, American Indian or Alaska Native, Asian, Native Hawaiian and Other Pacific Islander, both datasets for death rates were available only for total and the four races of White, Black, Asian or Pacific Islander, and American Indian or Alaska Native. Death rates for Native Hawaiians were not included in the necessary data. Consequently, the women who were assigned the numerical flag of Hawaiians in the demographics simulation were omitted from the cohort and no longer included in further studies.

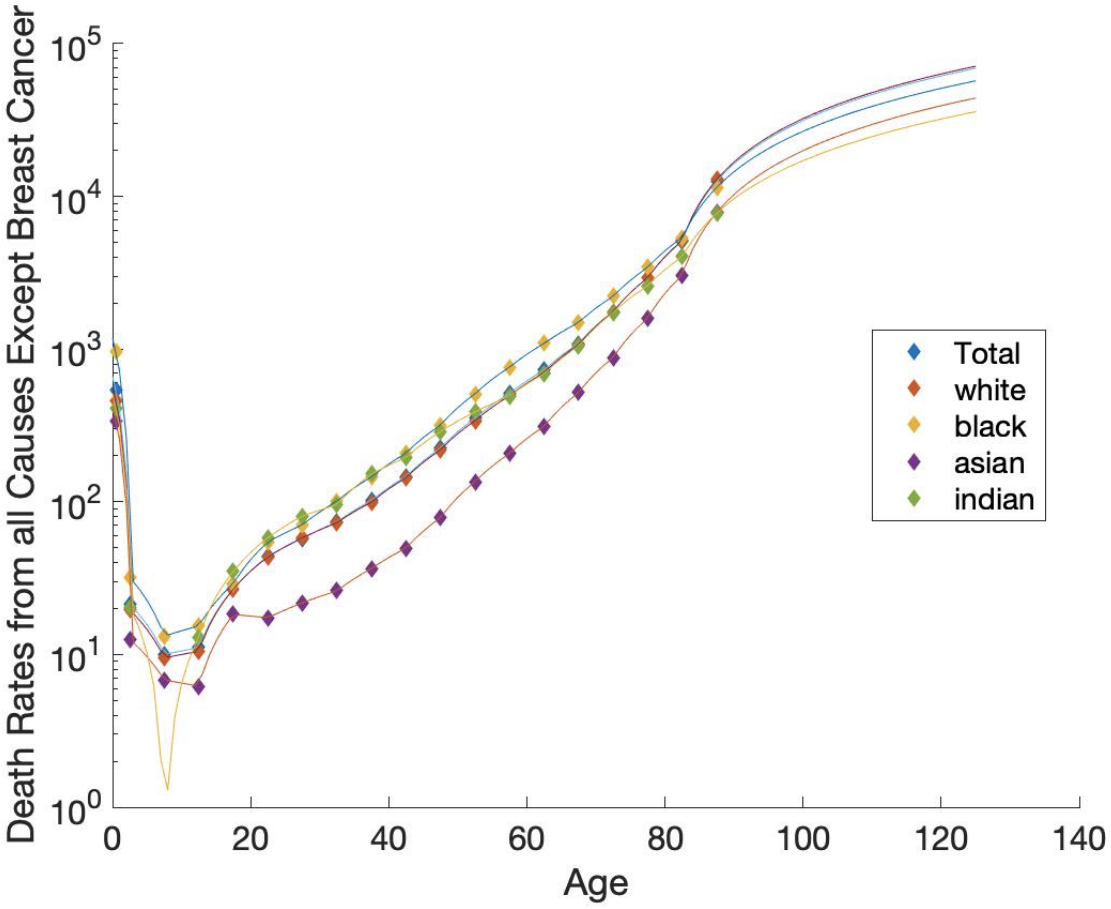

Fig 3.2.3 US Female Death Rates per 100,000 Population from all Causes Except Breast Cancer by Age and Race

The resulting dataset was modeled using the accept-reject method. Starting with the woman's age in 2016, assigned in section 3.1, the simulation lives through each woman's life until she reaches her age of death from non-breast cancer causes. Appropriate ages of death from non-breast cancer causes are assigned to the women in our generated cohort corresponding to their racial category.

Model Results

The results from the model are shown in figures 3.2.4 and 3.2.5. Figure 3.2.4 demonstrates the ages of death from all causes other than breast cancer for total and the four races of White, Black, Asian and Indian.

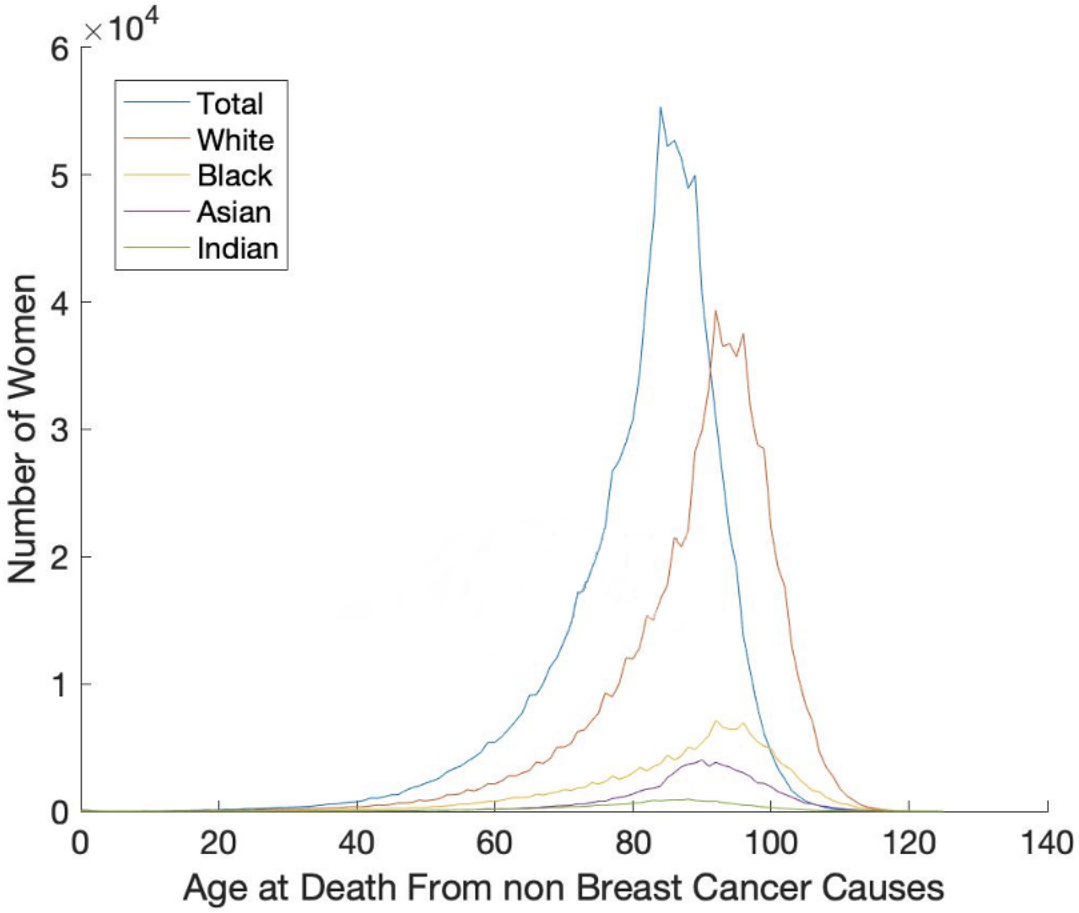

Fig 3.2.4 Death model results

Figure 3.2.5 shows a histogram of the ages of death from all causes other than breast cancer for all races as an example.

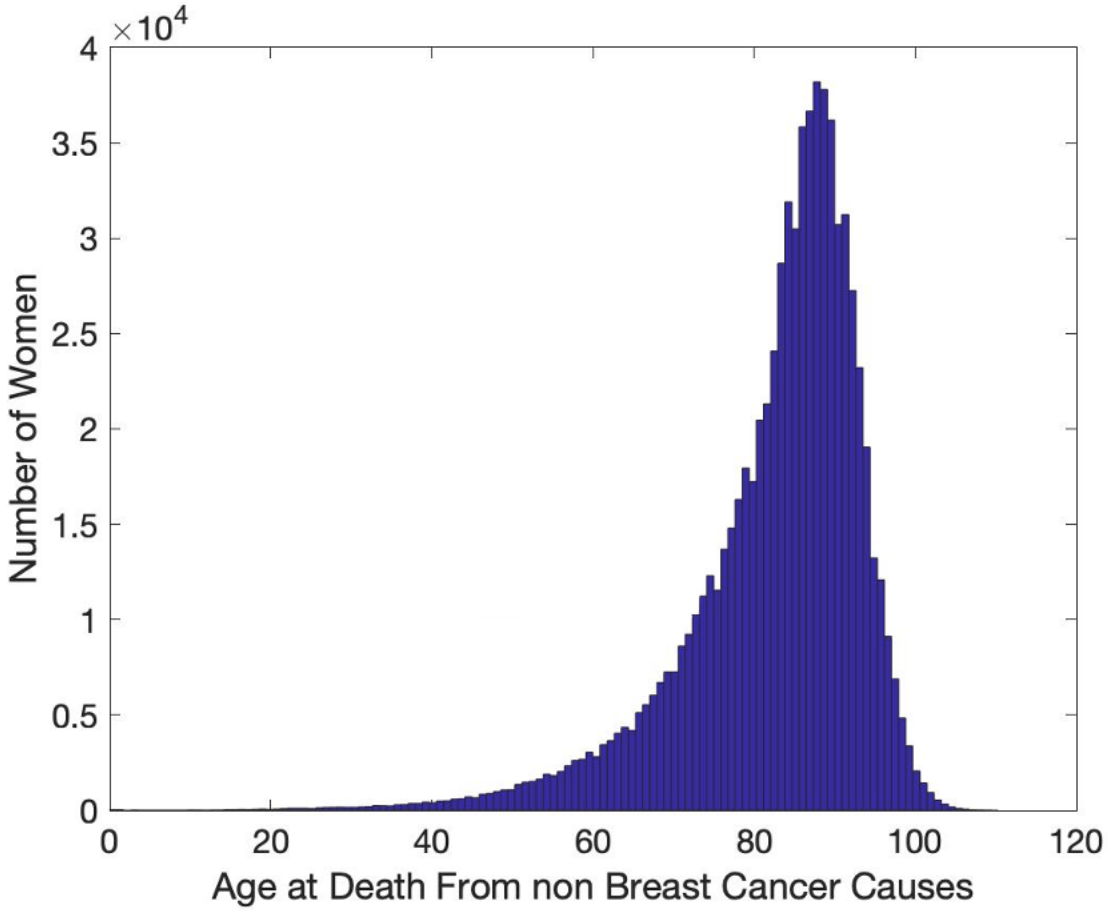

Fig 3.2.5 Histogram of Death Model Result for All Races

According to the CDC life expectancy for White females in the US is 81.1-83.8 depending on Hispanic origin. The average age of death for total in our model was 82.6 which is a good approximation.

A test to verify the death simulation was to calculate the death rates based on the ages of death assigned in the simulation to compare with the initial raw death rates. Figure 3.2.6 shows the result of this comparison for total per capita as an example. As can be seen, the plots match accurately and verify the simulation results.

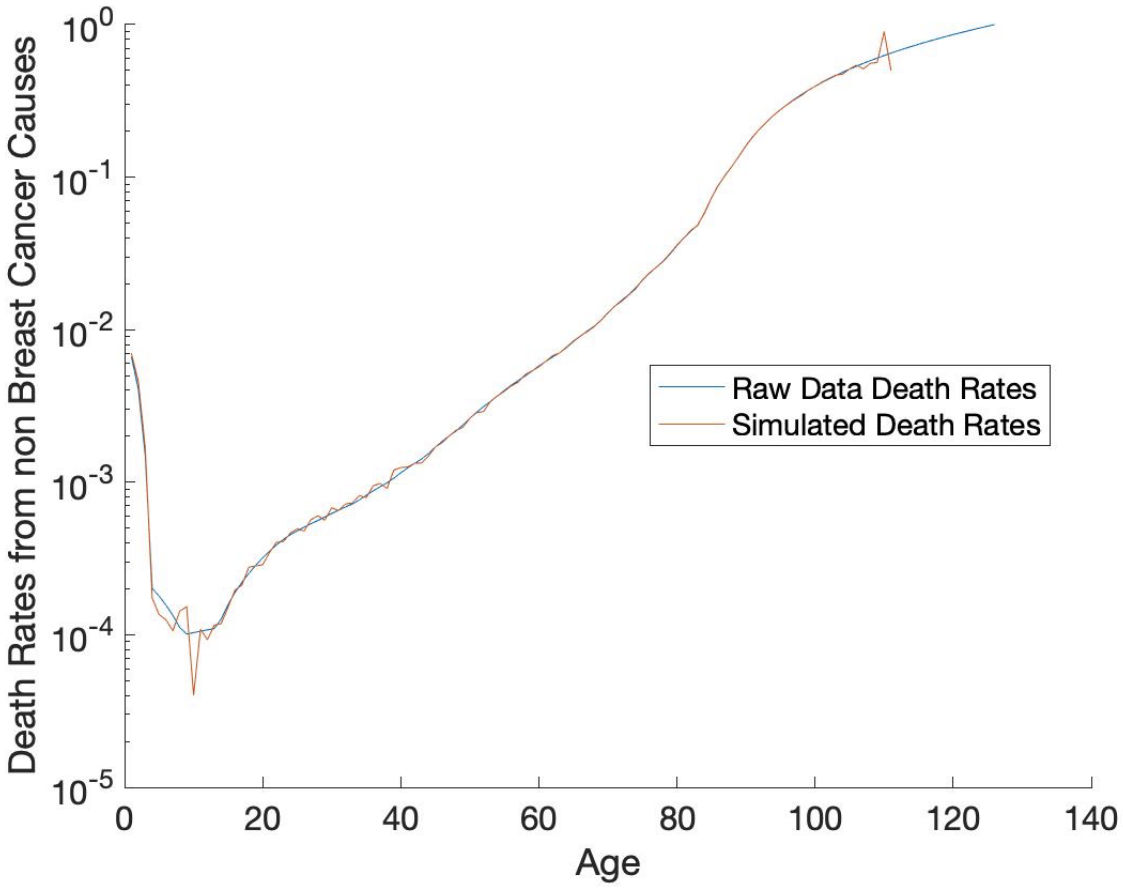

Fig 3.2.6 Death model Verification Results per Capita

As done for the demographics model, the five different cohorts of women generated and saved to our database were further studied to assess the variance and true randomness of the simulations. The death simulation was applied to each different cohort for comparison and the results were saved as another parameter component of each cohort. The resulting ages of death from non-breast cancer causes were compared and are shown for total (all races combined) in figure 3.2.7. The solid symbols illustrate the mean population of people dying at each age from all causes other than breast cancer and the error bars represent ±1 standard deviation (SD).

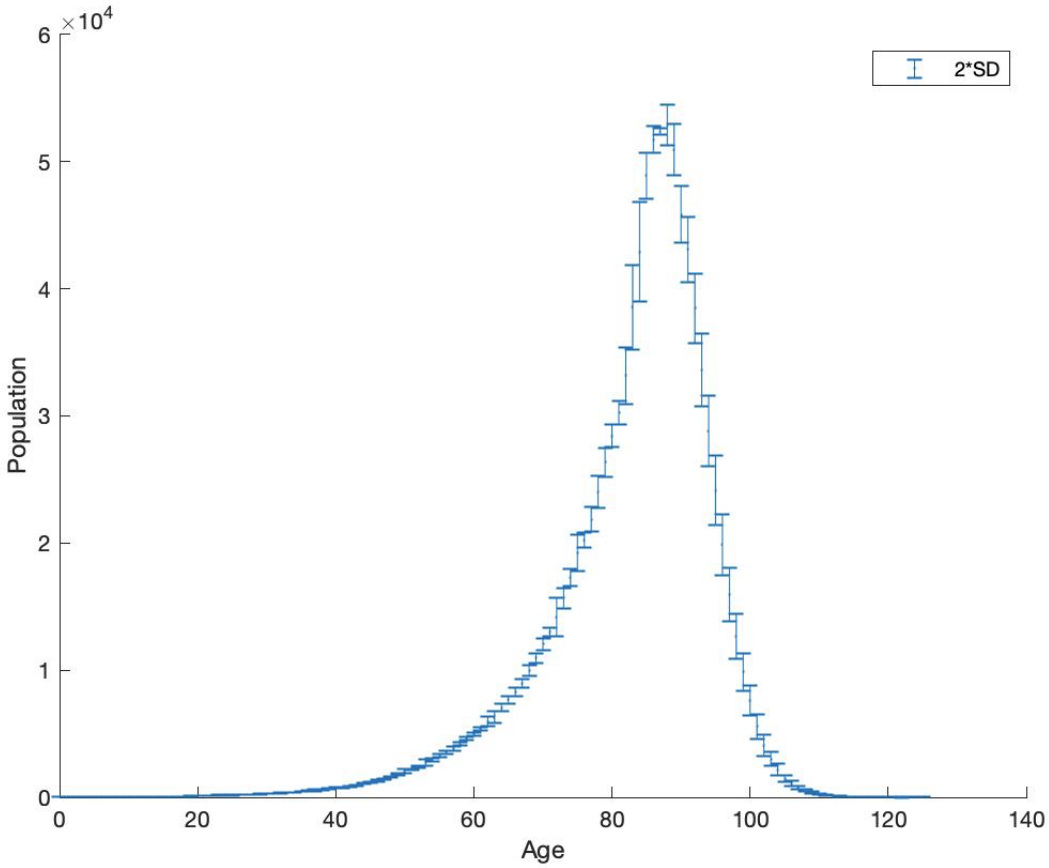

Fig 3.2.7 Death model Results

3.3 Incidence Model

Breast Cancer Incidence Data

The next step in generating the cohort was to determine the age at which each woman would contract breast cancer (if she does in her lifetime). In other words, the age of breast cancer incidence was another parameter assigned to each woman in the generated cohort. Data for breast cancer incidence rates by age was available on the Surveillance, Epidemiology, and End Results Program (SEER) website [53]. This data, shown in figure 3.3.1 includes breast cancer incidence rates for the US female population for all races combined and the four races of White, Black, American Indian or Alaska Native, and Asian or Pacific Islander. Hispanics and Non-Hispanics are not mutually exclusive from Whites, Blacks, Asian/Pacific Islanders, and American Indians/Alaska Natives. The rates are per 100,000 and this data is available at 5-year age interval resolution and people 85 and older are categorized as one age group. The data was interpolated to 1-year interval resolution which is included in the figure.

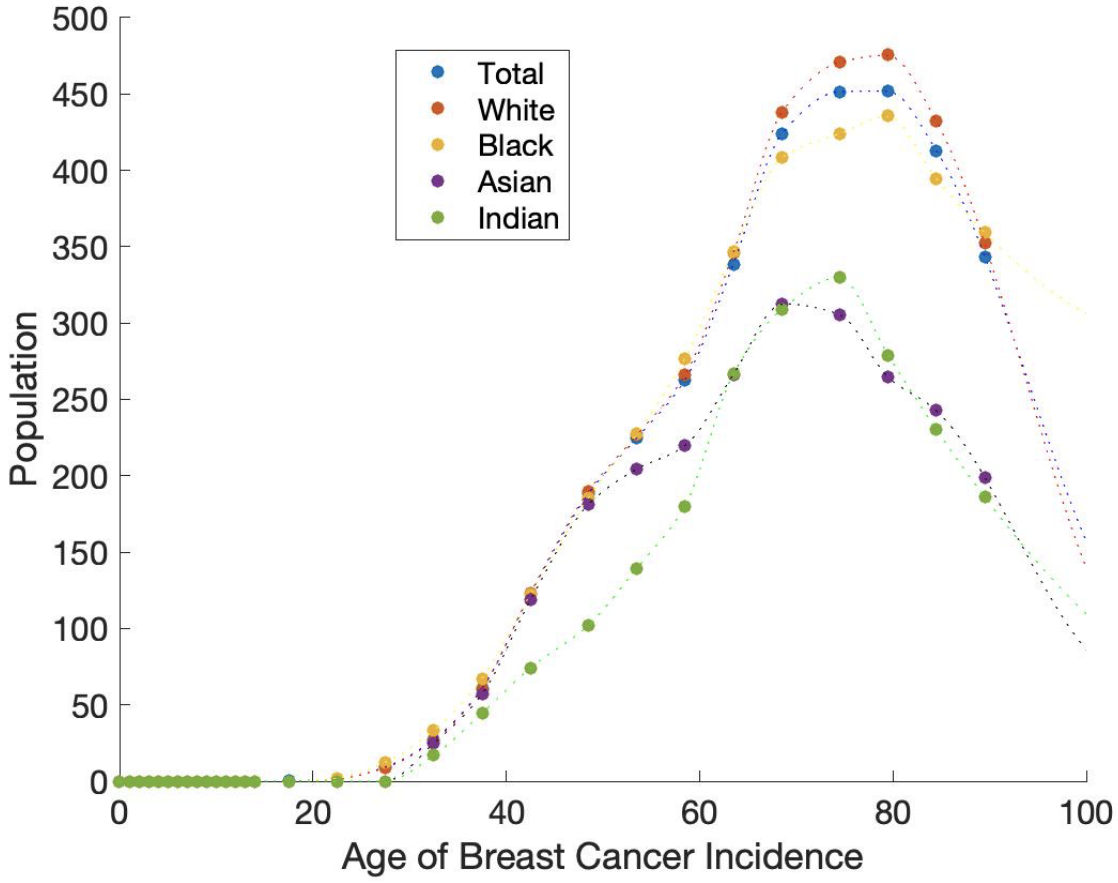

Fig 3.3.1 US Breast Cancer Incidence Rates per 100,000 by Age

Sojourn Time Data

The incidence rates shown earlier in fact reflect the time of detection as incidence. The time it takes for a tumor to be detected after it is initiated is called the Sojourn time (ST). Data for average breast cancer Sojourn time by age was available from Spratt et al. [54] This data, available only at 4 year intervals, and the interpolation can be seen in fig 3.3.2.

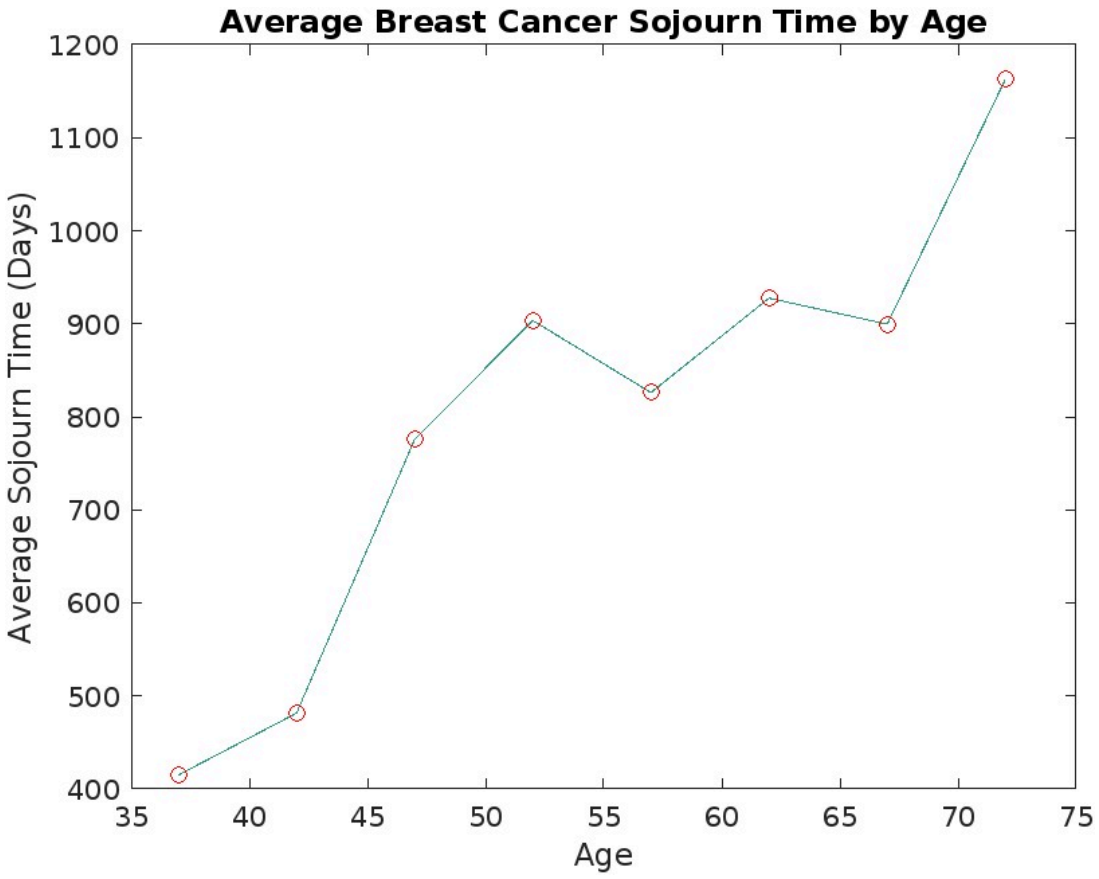

Fig 3.3.2 Average Breast Cancer Sojourn Time by Age

Incidence Model Methods

Using the interpolated age-dependent Sojourn time data we adjusted the incidence rates backwards in time to reflect the incidence at the time the tumors are initiated. Thus, the true age of breast cancer incidence or initiation, the original (SEER) incidence rates and the resulting Sojourn time-corrected incidence rates are shown in figure 3.3.3. As illustrated, the rates have shifted towards younger ages of incidence.

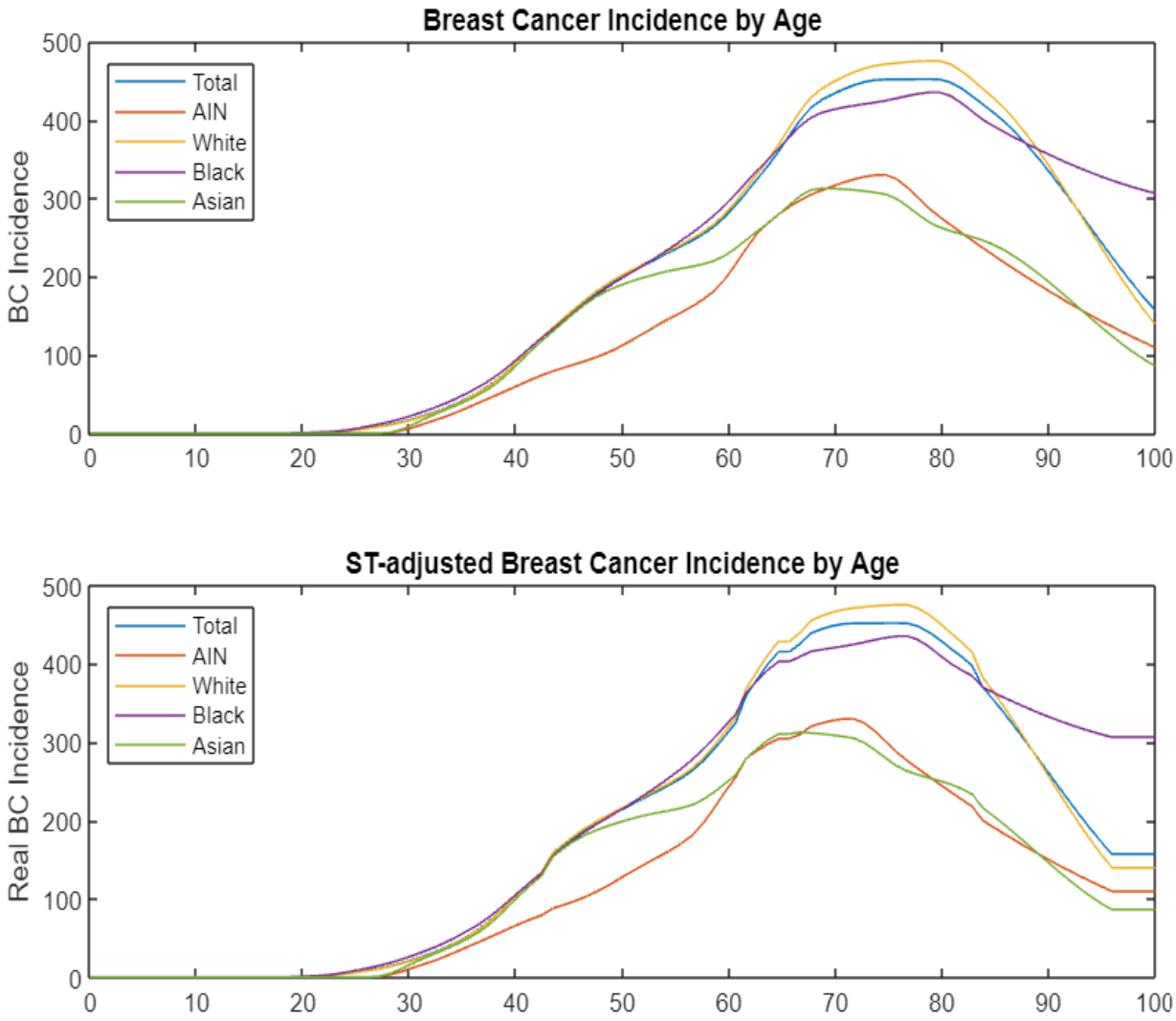

Fig 3.3.3 SEER Breast Cancer Incidence Rates and Sojourn-time Corrected Incidence Rates

Model Results

The results from the model are shown in figures 3.3.4 and 3.3.5. Figure 3.3.4 demonstrates the ages of breast cancer initiation for total and the four races White, Black, Asian, and American Indian or Alaska Native. Figure 3.3.5 shows a histogram of the ages of breast cancer initiation for total. The average age of breast cancer initiation for total is approximately 68 years old.

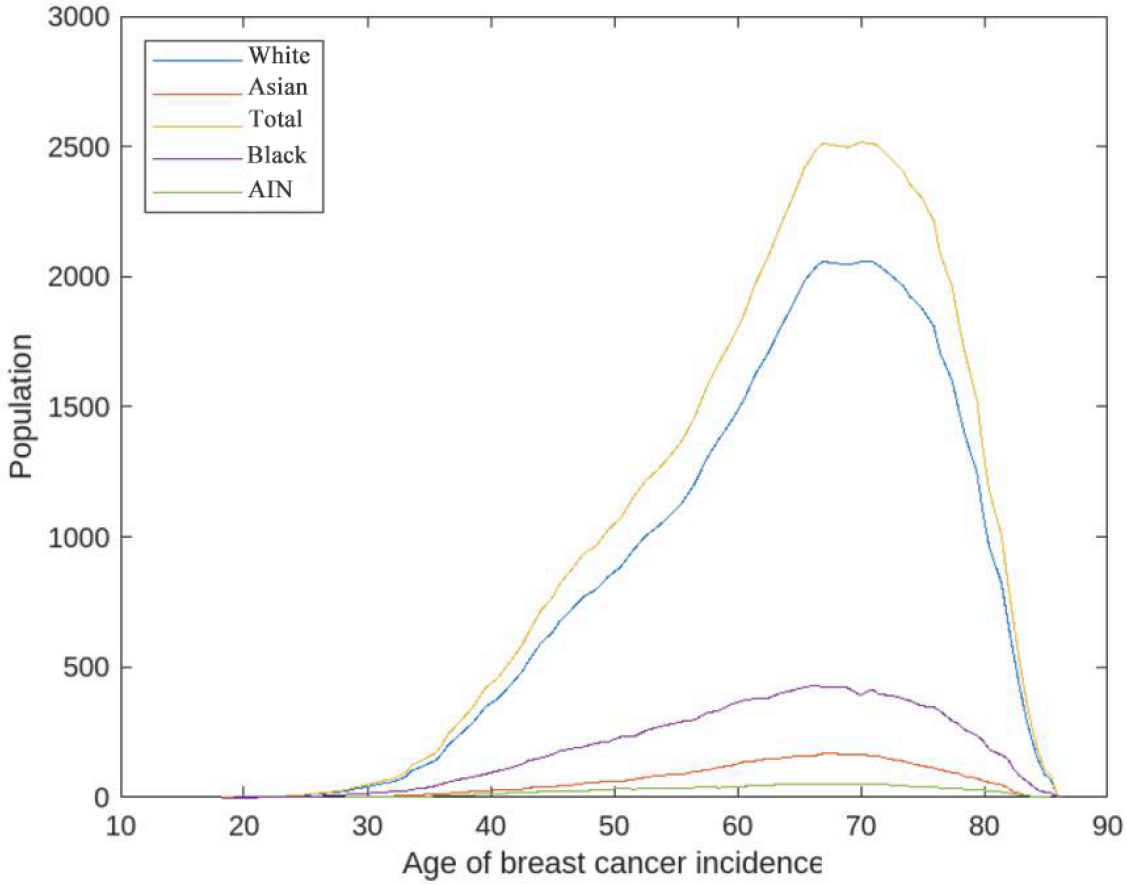

Fig 3.3.4 Breast Cancer Incidence Model Results

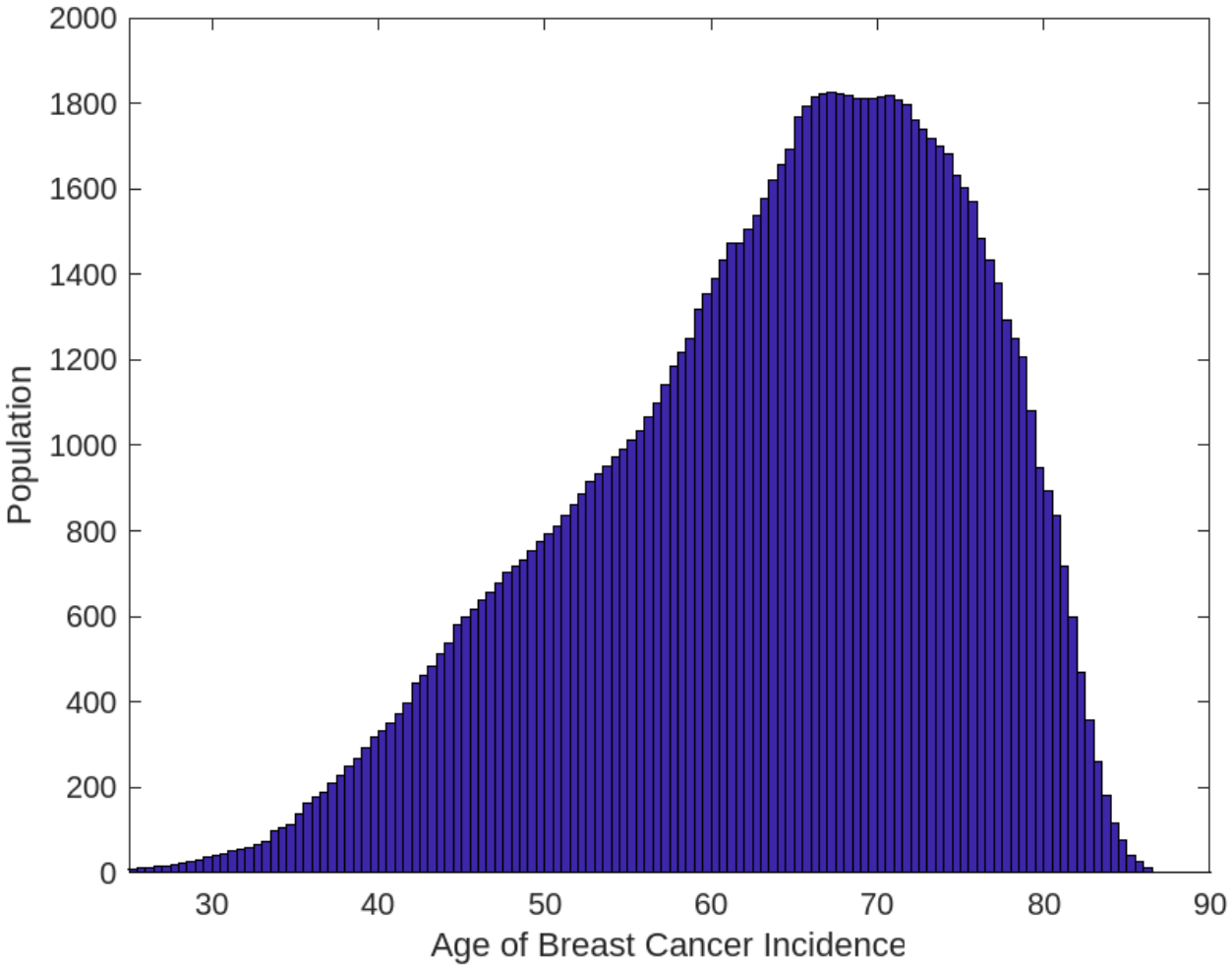

Fig 3.3.5 Breast Cancer Incidence Model Result for Total

A method to verify the incidence simulation was to calculate the incidence rates based on the ages of incidence assigned in the simulation to compare with the initial raw incidence rates. Figure 3.3.6 shows the result of this comparison for total per capita as an example. As can be seen, the plots match accurately and verify the simulation results.

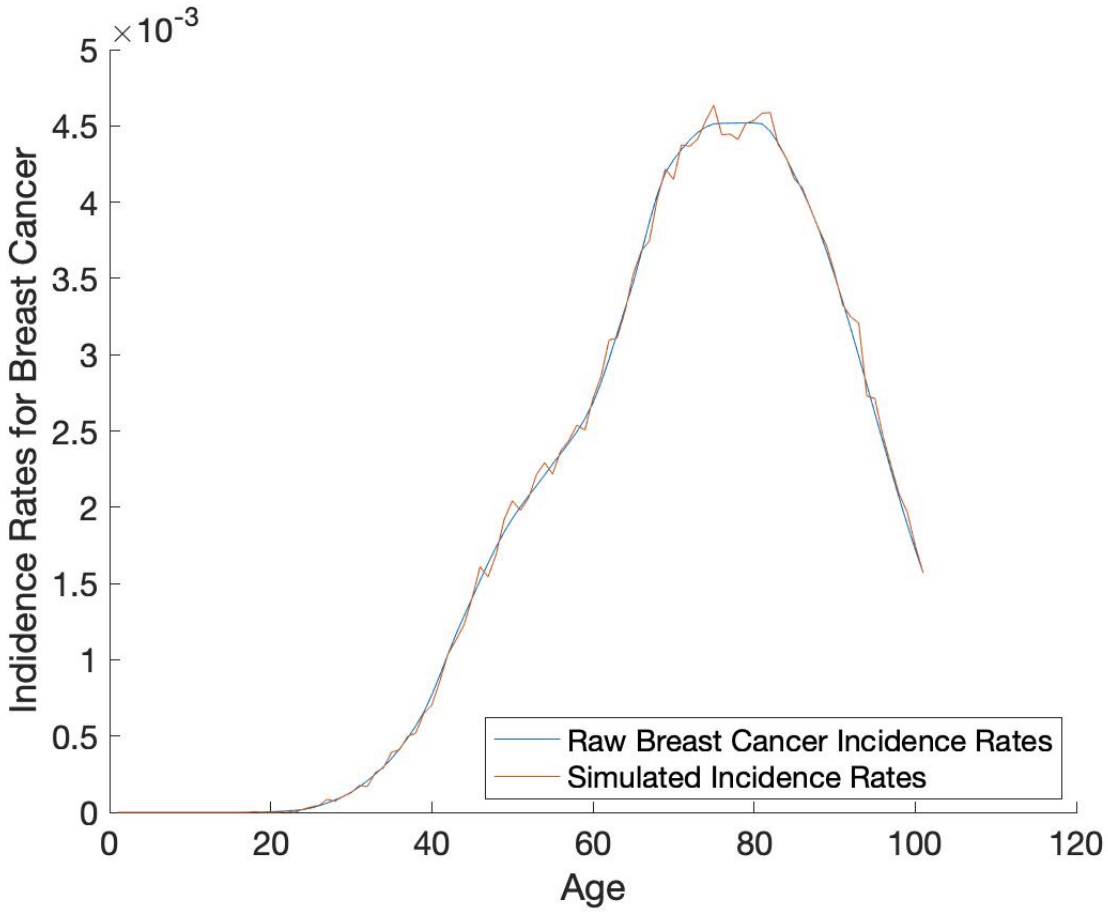

Fig 3.3.6 Breast Cancer Incidence Model Results and Raw Data for Total (All Races Combined) per Capita

As done for the earlier models, the five different cohorts of women generated and saved to our database were further studied to assess the variance and establish the true randomness of the simulations. The incidence simulation was applied to each different cohort for comparison and the results were saved as another parameter component of each cohort. The resulting ages of breast cancer incidence were compared and are shown for total (all races combined) in figure 3.3.7. The solid symbols illustrate the mean population of people contracting breast cancer at each age and the error bars represent ±1 standard deviation (SD).

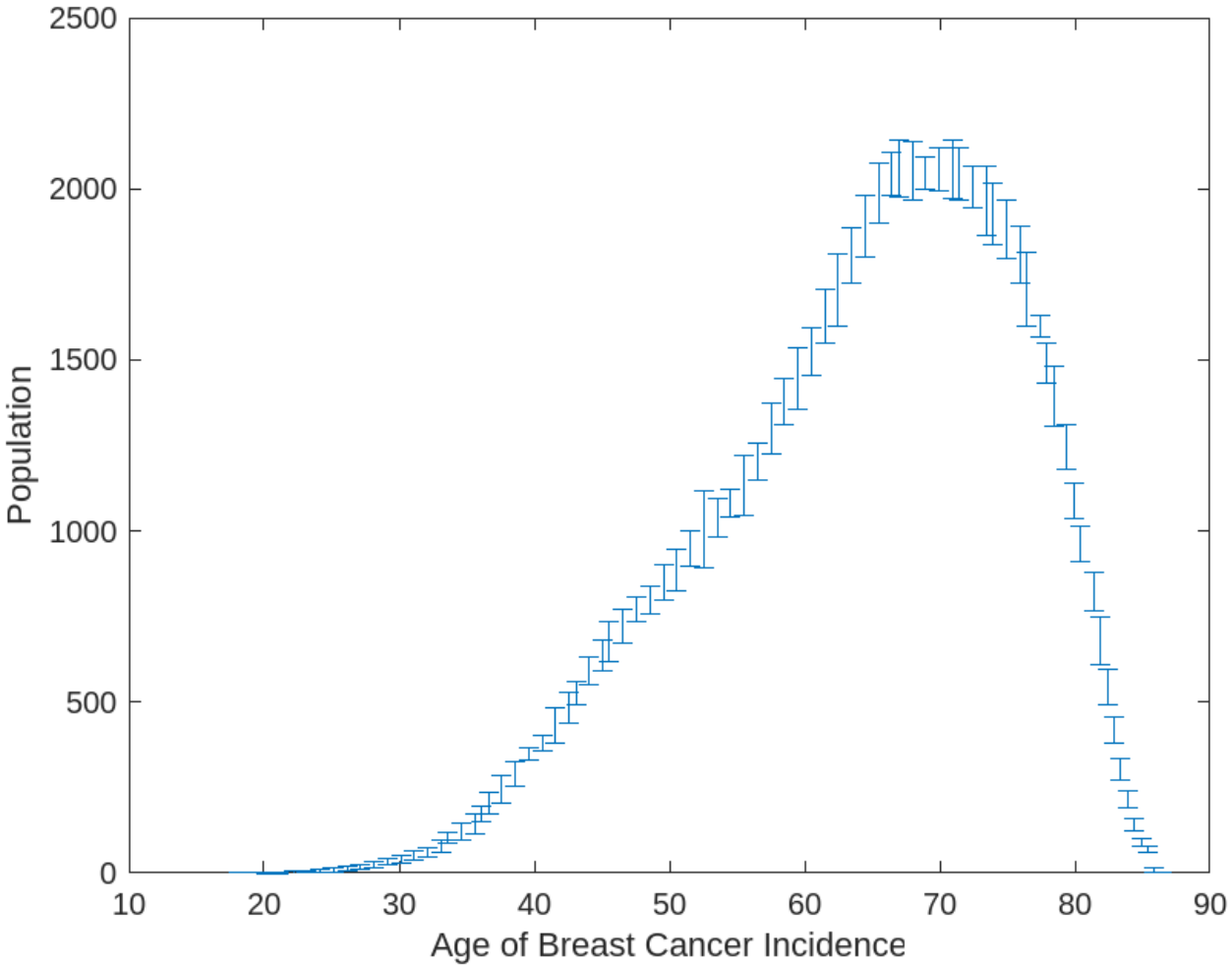

Fig 3.3.7 Breast Cancer Incidence Model Result for Total

3.4 Breast Cancer Growth Model

Breast Cancer Growth Rates

Based on Fornvik et al [55], the Gompertzian model of breast cancer growth is of the form that follows:

$$V(t) = a \times e^{-b \times e^{-k \times t}}$$

Where t is time, k is the growth rate, a is the asymptote, and b sets the displacement on the time axis. In this model, the breast tumor is assumed to have a spherical shape. Coefficient a, the asymptote, is set to be $14137 mm^3$, the volume of a $30 mm$ diameter tumor because the breast cancer growth rates approach $30\ mm$ diameter at the end of the growth curves. The value for coefficient b is calculated by setting the volume of the tumor at the beginning i.e.

time zero equal to the volume of a single breast tumor cell. Based on Spratt et al [54] the volume of a single breast cancer cell is $10^{-6}mm$ thus setting b equal to 23.37206131:

$$V(t=0) = a \times e^{-b \times e^{-k \times 0}} = a \times e^{-b} = 10^{-6}mm \Rightarrow b = 23.37206131$$

Dahan et al [56] define tumor doubling time (DT) as the time in days it takes a tumor volume to double in size. Data from Michaelson et al [57] was used to obtain the growth rate (k) values. Taken from Peer et. al [58], the paper had the values for DT of three breast cancer incidence age groups. The doubling times shown in table 3.4.1 were assumed to be the doubling times for 45-, 60- and 80-year-old women respectively.

Age Group	<50	50-70	>70
DT	80 days	157 days	188

Table 3.4.1 Breast Tumor Doubling Time by Age

Considering the aforementioned DTs are for a 5 mm diameter tumor, using the definition of doubling time and the Gompertzian model of breast cancer growth rates, the growth rate (k) values corresponding to each of the three DT values were calculated.

$$V(t+DT) = 2V(t), V(t) = a \times e^{-b \times e^{-k \times t}} = 4/3 \times \pi \times (5/2)^3$$

$$\Rightarrow k = -ln\,(1 - ln\,2/(3 \times ln6))/DT$$

The results $k1 = 0.001725712159610, k2 = 8.793437755974515 \times 10^4, k3 = 7.343455998340420$ corresponding to each age were then interpolated by Excel to a power fit to obtain the growth rates for all ages. The result was the following relationship:

$$k(a') = 0.0674 \times (a')^{-1.042}$$

where a' is the age of the woman at breast cancer incidence.

Using the resulting growth rate by age relationship along with the Gompertzian growth model we were able to obtain the breast cancer growth curves by age as seen in figure 3.4.1

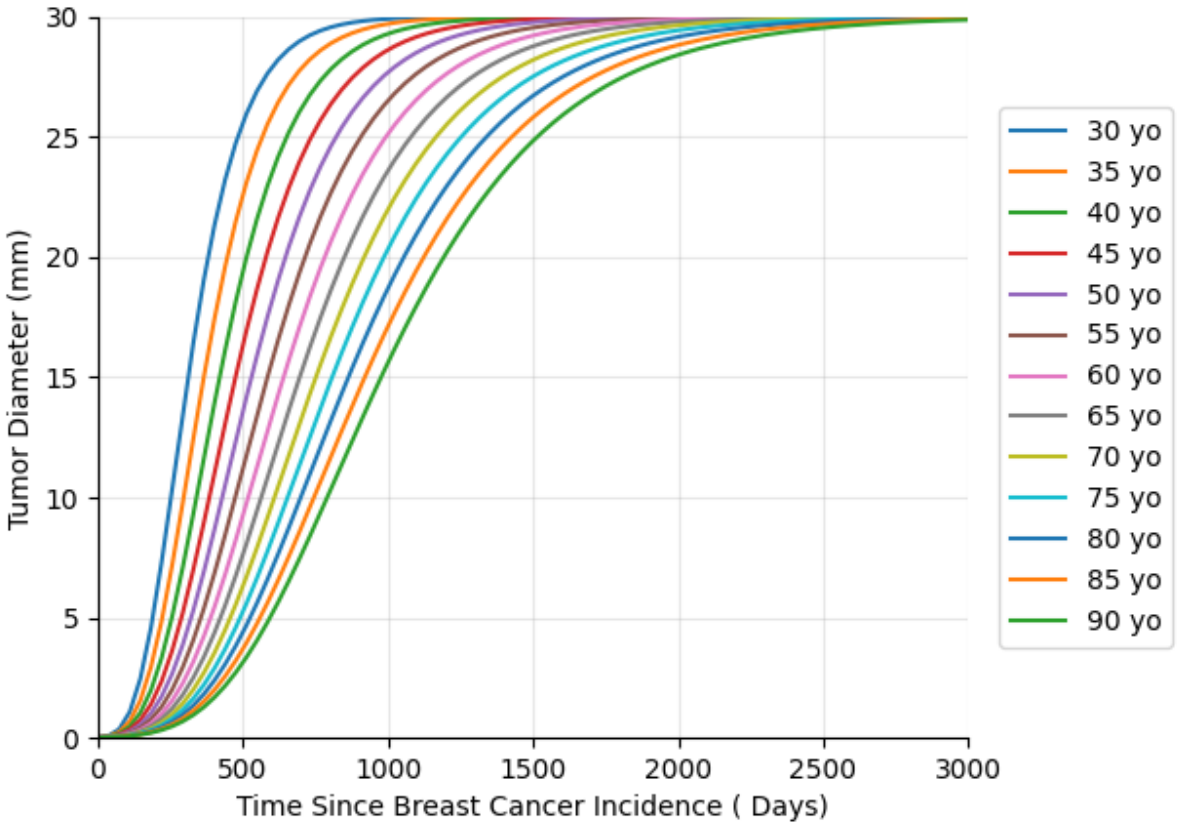

Fig 3.4.1 Breast Cancer Growth Curves by Age

Assigning the growth rate factor to each woman concludes the cohort generation part of the project. To sum up, a cohort of 1000000 women with 5 parameters was generated. The 5 parameters assigned were the age of the woman in the year 2016, the code for racial background, age of death from all causes excluding breast cancer, age of breast cancer incidence, and the breast cancer growth rate. The next step in the project was developing the breast cancer screening model.

4 Breast Cancer Screening Model

As mentioned earlier, the next step of the project was to develop a screening model. This screening model would then be applied to the cohort generated in chapter 3 and further studied. The screening model itself consists of two sections. First, a model for the detection was developed, the results of which were then used in a model for survival.

4.1 Breast Cancer Detection Model

Detection Probability Data (Screening Sensitivity)

Detection of breast cancer based on lesion diameter was studied. The study concentrated primarily on Projection Imaging or mammography and Computed Tomography (CT). Another possibility studied was if no breast cancer screening was performed in which case the tumor would eventually be discovered through palpitation or breast self-examination (BSE). A model was developed for the detection of breast cancer.

The probability of detection by each modality is indicated by the sensitivity of the screening modality. Sensitivity rates for mammography and breast CT were used in developing the detection model. The sensitivity rates data was available from Chen, L, et al [59]. This data, shown in Figure 4.1.1, illustrates the probability of breast cancer detection by mammography and CT by spherical lesion size. The spherical lesion size is the lesion diameter in mm.

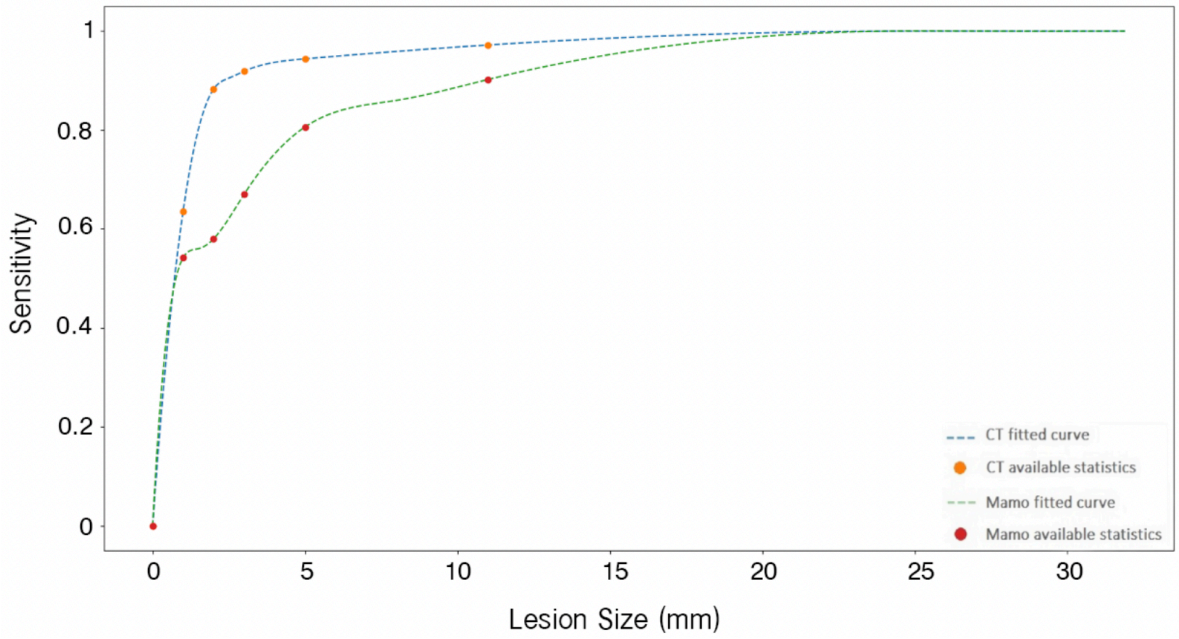

Fig 4.1.1 Sensitivity Rates by Lesion Diameter Data and Interpolations

As shown in the plots, limited data points were originally available. The software Tablecurve 2.0 was used to determine the most accurate interpolation trends for the sensitivity rates. As seen, Figure 4.1.1 illustrates the original data along with the interpolations for both CT and mammography. It can be gathered that CT is considerably more accurate and efficient than mammography.

In case of no screening or BSE, the tumor would get detected after reaching a palpable size. That size is generally considered to be 21.5mm diameter [60, 61] which was used as the threshold for tumor detection by BSE in our simulation. Based on the growth rates specific to each woman, her tumor would reach the threshold size at an age specific to her determined by the growth model.

Methods

The data above was then implemented into a detection simulation. Using rejection sampling, probability of detection as a function of tumor size, and the breast cancer growth model we were able to determine at what point in time the tumor would get detected by each modality.

The screening model consisted of three variables: screening start age, screening end age, and screening frequency. An example of a screening regime performed was screening start time at age 40, screening end time at age 80, and screening time interval of 1 year. This meant that any woman older than 40 years old and younger than 80 years old would be tested every year through the screening program. Different regimes were developed and studied by assigning different values to these 3 parameters which will be discussed in more detail further in Chapter 5.

As each woman ages and reaches the screening start age, she would undergo regular screenings as frequently as set by the screening interval parameter. Meanwhile, the person's cancer would be growing at the rate determined by the growth factor assigned to her starting at the age of her cancer incidence. Therefore, the size of the tumor is known at each point in time. At each screening, the detection simulation looks up the sensitivity rate for a tumor of the respective lesion size to determine the probability of detection at that screening time. Utilizing the accept-reject method at this point, if the tumor gets detected that would be the age of her cancer detection. If the tumor does not get detected at this round of screening, she will continue to undergo screening until it does.

If the tumor does not get detected by CT or Mammography it can be detected with BSE after the tumor reaches the 21.5 mm cutoff diameter. While BSE is not a screening method, the same screening interval as used for CT and Mammography was used for consistency. This frequency affects the exact time the tumor is found after it reaches 21.5mms. For some people, the tumor never gets detected with screening or BSE because they would reach their age of death prior to the age at which their tumor would be detected.

Results

As expected from the sensitivity data, the tumors were detected at younger ages and smaller sizes with CT compared to Mammography. No screening was the least efficient and led to detection at larger sizes or older ages. The results of different screening regimes are discussed in more detail in chapter 5.

Figure 4.1.2 shows histograms of lesion size at the time of detection for yearly screening starting at age 40 and ending at age 80 for each modality. As illustrated, lesion sizes at detection are concentrated at higher sizes with BSE, spread out with Mammography, and most concentrated at lower sizes with CT. The average lesion size at detection was 8 mm with CT and 13 mm with Mammography. This result is compatible with the average lesion size at detection in Shaevitch et.al.[62] As mentioned earlier in the growth model, breast tumors approach 30 mm diameters with time. This explains the relatively significant population whose cancer gets detected at 30 mm diameter. Because breast cancer growth rates are higher at younger ages tumors of most people who contract breast cancer at younger ages reach 30 mm before screening starts which leads to detection lesion size of 30 mm for all of this population.

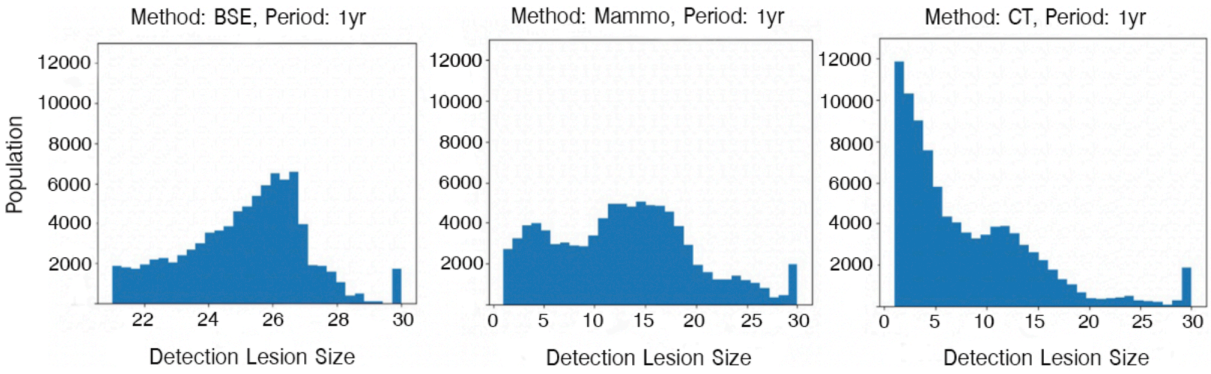

Fig 4.1.2 Histogram of Lesion Size at Detection for Total
with Screening Start Age of 40 and End Age of 80 at 1 Year Intervals

A test to verify the detection model was to calculate the sensitivity rates based on the ages of detection assigned in the simulation to compare with the initial sensitivity rates data. Figure 4.1.3 shows the result of this comparison for total as an example. As can be seen, the plots match accurately and verify the simulation results.

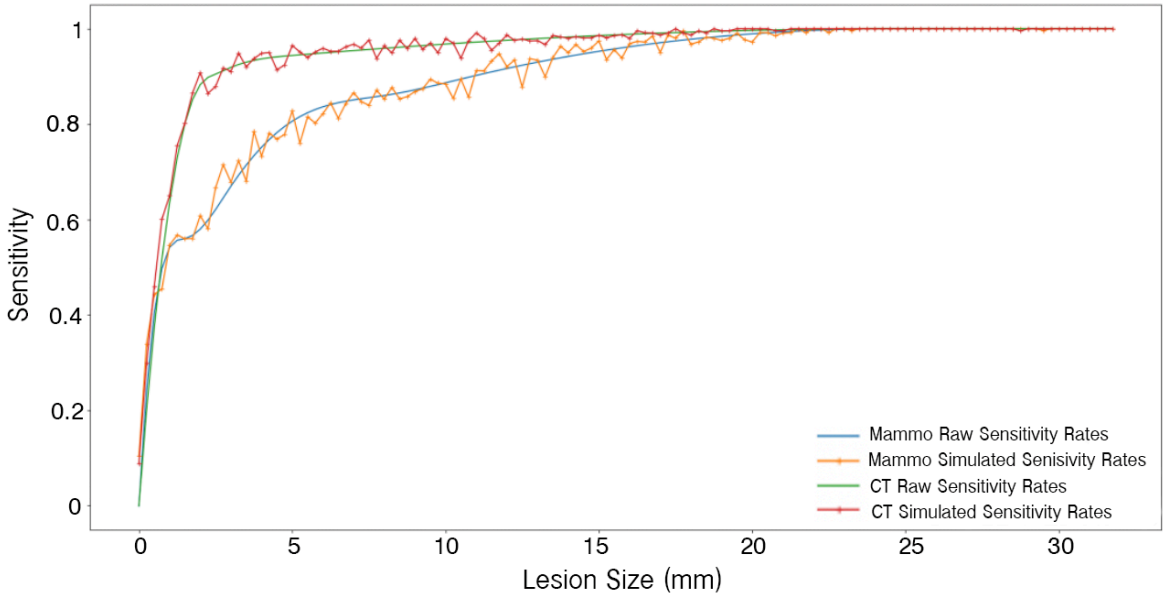

Fig 4.1.3 Detection Model Results for Total

As done for the earlier models, the five different cohorts of women generated and saved to our database were further studied to establish the true randomness of the simulations. The detection simulation was applied to each cohort for comparison and the results were saved as another parameter component of each cohort. The result of this comparion is shown in figure 4.1.4 for total (all races combined). The solid symbols illustrate the mean sensitivity rates at each tumor detection size and the error bars represent ±1 standard deviation (SD).

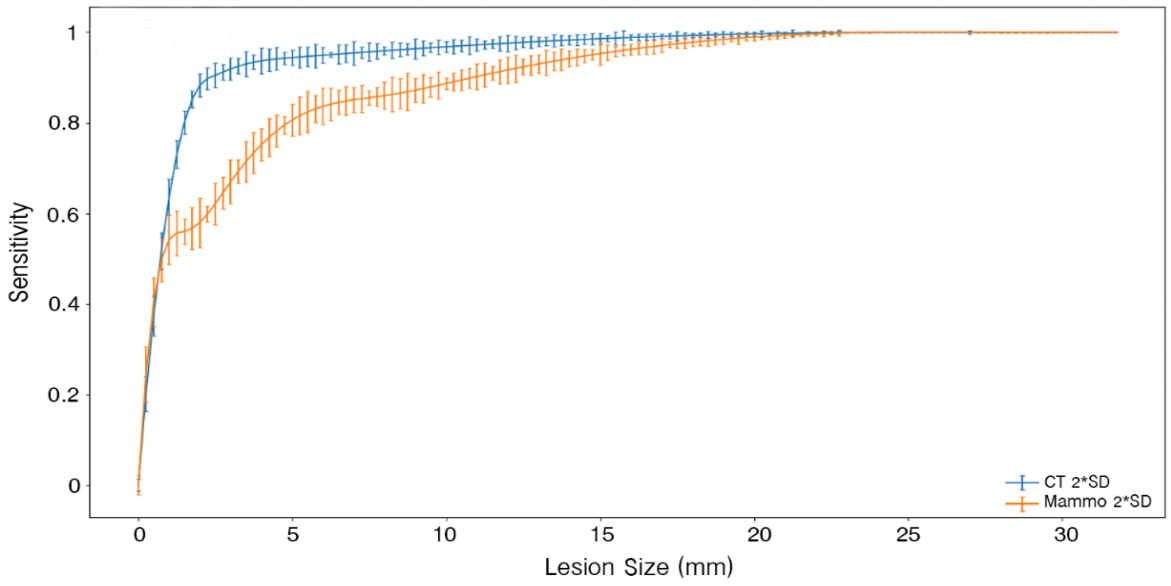

Fig 4.1.4 Breast Cancer Detection Model Results for Total

4.2 Breast Cancer Prognosis Model (Survival)

The purpose of breast cancer screening is to identify women who have contracted breast cancer. These women suffer the risk of dying from breast cancer in addition to the risk of death from other causes. Hence, after detection, the next step of the screening model was to determine the prognosis. A comprehensive review of the recent literature on breast cancer prognosis was conducted, and a model was developed for survival. The prognosis model takes into account the woman's age, race, and the size of breast cancer at detection.

Breast Cancer Prognosis (Survival) Rates Data

The most accurate data for prognosis is from long-term follow-up population research which reflects the prognosis of treatments common in the 1960-1980s. While new and improved breast cancer treatments lead to a better prognosis, long-term studies on the newest treatment regimens would not be available for many years. Thus, our model incorporates the best prognosis data currently available.

Survival data from Michaelson et. al [63] was used to develop the prognosis model and built into a lookup table. The data available was the probability of survival by time since diagnosis in the range of 0-15 years for five categories of tumor diameter. The size categories included 10-14, 15-19, 20-39, and above 50 mm tumor diameters. As seen in figure 4.2.1 this data was assumed to be the probability of survival for the median of the diameter range of each category instead of the whole range of the categories, meaning the plots shown in figure 4.2.1 were assumed to be the survival for a 12, 17, 24.5, 39.5 and 55mm diameter tumor. In other words, the survival rate indicated for each group was assumed to be the survival for the median of the diameter range of that category as a representative of that group. A survival rate of 100% for a 0 mm tumor was also added to the data points, as seen in the figure.

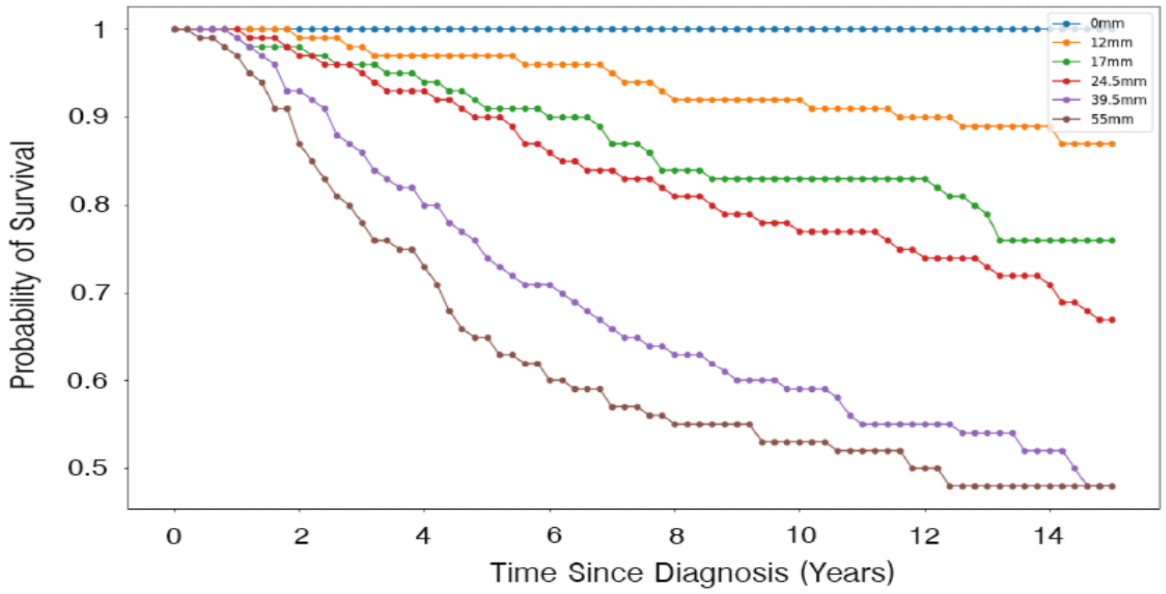

Fig 4.2.1 Breast Cancer Survival Rates

Prognosis Model Methods

Data from the previous plot was extracted using Microsoft Excel. This dataset was then interpolated with MATLAB to obtain the probability of survival for tumors of all sizes as seen in figure 4.2.2. The interpolation was done in 1 mm intervals, thus yielding the survival rates for 1, 2, 3, …, 55 mm tumors which was sufficient resolution for the purposes of this study.

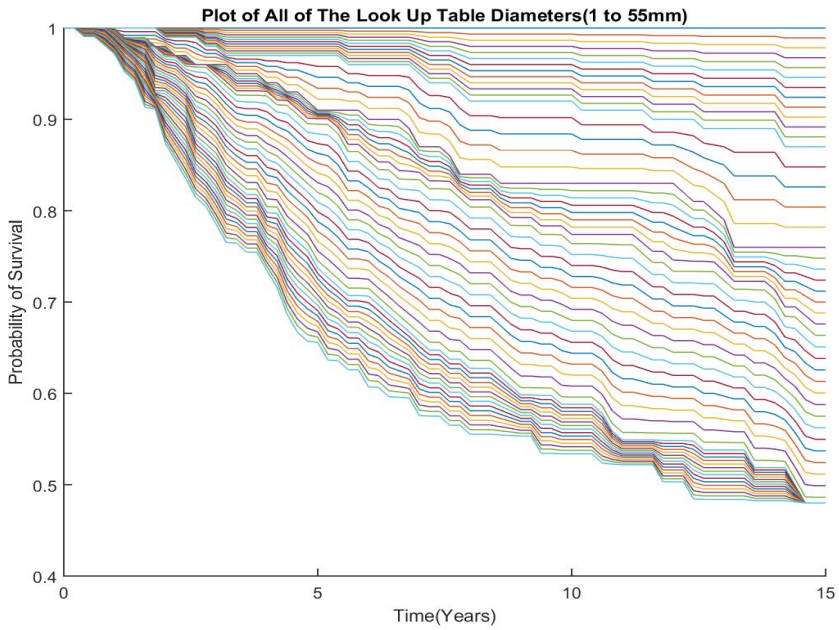

Fig 4.2.2 Interpolated Breast Cancer Survival Rates

Using the growth rates, ages at detection determined in the previous section, and survival rates we were able to obtain the probability of breast cancer survival at each point in time in the woman's life since detection.

For the prognosis after detection, the survival data was used to determine whether the patient died from breast cancer or other causes, and if she died from breast cancer to determine the time of death from breast cancer. As seen in figure 4.2.3, the probability of a woman dying from breast cancer before she dies of a non-breast cancer cause (p) is $p = D/(D + L)$. D is the area under the survival curve from $t = 0\ to\ t = Tdeath$, L is the area above the curve and $Tdeath$ is the time of death from non-breast cancer causes. Because we know the age at detection and the age of death from non-breast cancer causes, $Tdeath$ can be easily calculated by subtracting the two for each woman.

A random number r was generated and compared with p for each woman to determine if she survived breast cancer or not. Rejection sampling was then used to figure out the time at which the woman dies of breast cancer if she dies of breast cancer before she would die of a non-breast cancer cause.

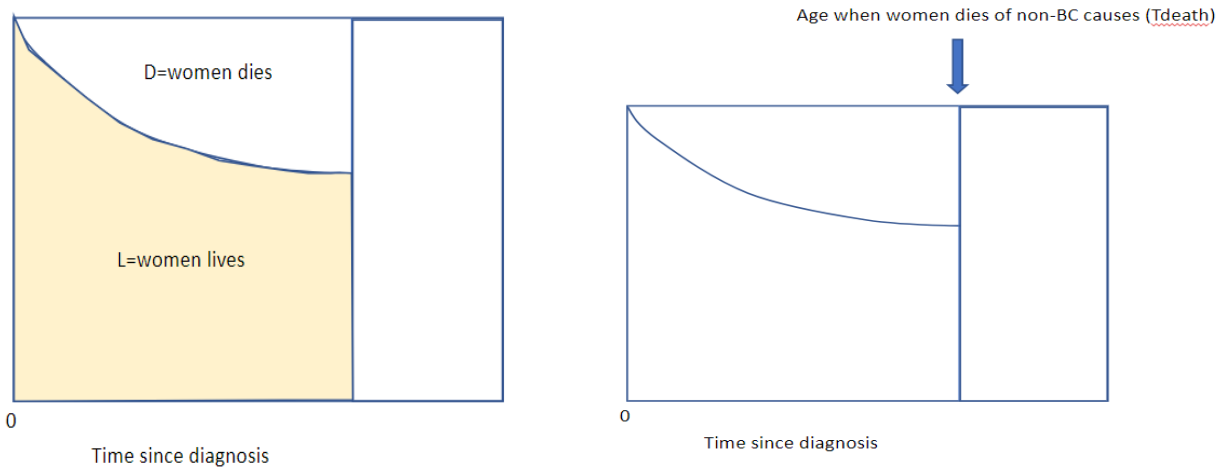

Fig 4.2.3 Breast Cancer Prognosis Model Scheme

Prognosis Model Results

To verify the prognosis model, survival rates based on ages of death assigned in the simulation were compared to the initial raw survival rates. The result of this comparison is shown in figure 4.2.4 for all races combined.

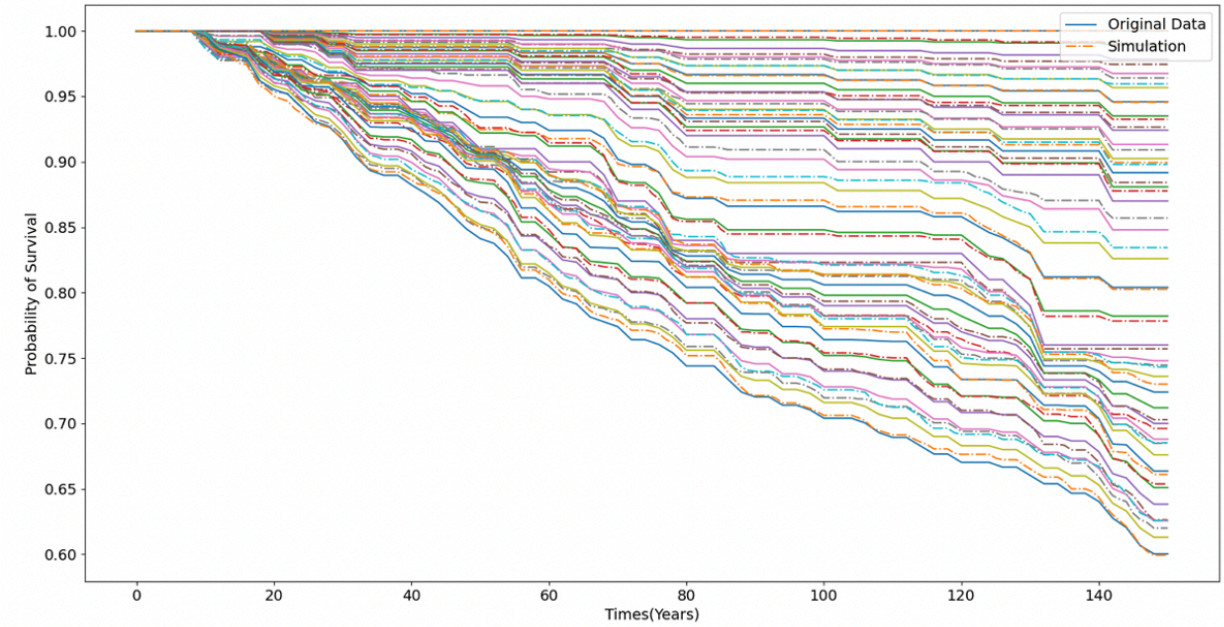

Fig 4.2.4 Breast Cancer Prognosis Model Results

As done for the previous models, the five different cohorts of women generated and saved to our database were studied with the survival model to establish the true randomness of the simulations. The results were compared and are shown for total (all races combined) in

figure 4.2.5. The solid symbols illustrate the mean survival rates, and the error bars represent ±1 standard deviation (SD).

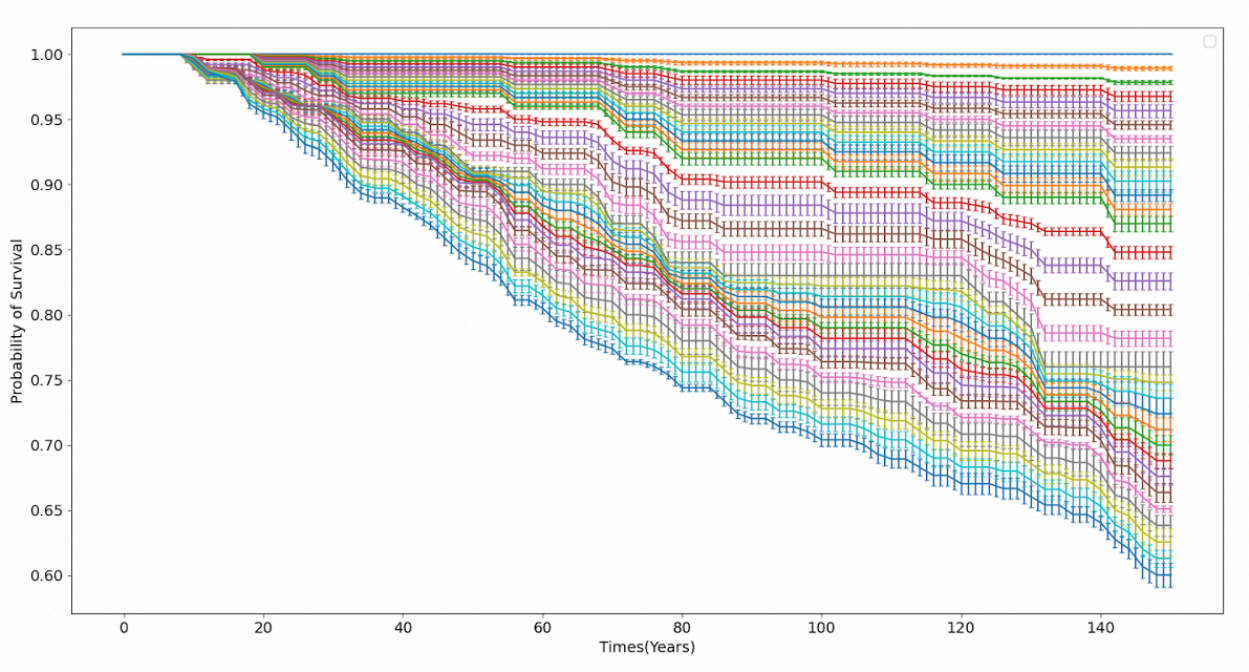

Fig 4.2.5 Breast Cancer Prognosis Model Results

5. Results

After the screening simulation was developed, different screening regimes were tested and studied. The regimes to explore were studied with breast CT, mammography, and no screening or breast self-examination (BSE). The regimes differed in screening start age, end age, and screening intervals in addition to the modalities used. Several parameters of interest resulting from each regime were studied and used in comparisons to determine the most efficient regime. The different regimes and parameters of interest will be explained in more detail in this chapter.

The different screening start and end ages included screening 40- to 80-year-olds, screening from age 40 to end of life, screening starting at age 50 and ending at age 80, and screening from age 50 to end of life. Screening at 1-year, 2-years, 3-years and 4 years intervals were explored.

The parameters of interest were the size of the lesion (in mm – diameter) at the time of detection, histogram of the lesion size at the time of detection, years of life saved, years of life saved as a function of the age of the patient at the time of breast cancer detection, and years of life saved per the number of exams performed. These five parameters were computed for each regime in order to conduct the required comparisons.

5.1 Lesion Size at the Time of Detection

A parameter of interest was the size of the lesion (in mm diameter) at the time of detection. As expected from the sensitivity rates in section 4.1, on average size at detection was lower for CT than mammography and highest for no screening (BSE). Averaged over all screening regimes the average size of the lesion at the time of detection was 3.4 mm smaller with CT (16 mm) than with mammography (19.4 mm). The average size of the lesion at the time of detection was 25 mm for BSE.

Among the different screening regimes for CT and mammography screening starting at age 40 until the end of life had the lowest average size of lesion at detection and screening from age 50 to 80 with mammography had the highest lesion size at detection. The difference between screening ages 40 to 80 and 40 to 125 or 50 to 80 and 50 to 125 was slight. Lesion size at detection differed very slightly among different races. The difference between average sizes at detection with CT and Mammography lowers with higher screening intervals. This was expected as the difference between sensitivities of the two modalities is higher at lower sizes and the time elapsed from tumor incidence until detection is lower with higher screening frequency which leads to smaller tumor size at detection on average.

average lesion size at the time of detection (mm)								
screening intervals (years)	CT (40-80)	mamo (40-80)	CT (50-80)	mamo (50-80)	CT (40 -125)	mamo (40-125)	CT(50-125)	mamo (50-125)
1	8.1	13	10.1	14.4	8	12.8	9.7	14.0
2	14.1	18	15.5	19.1	14	17.8	15.1	18.7
3	18.5	21.4	19.4	22.2	18.4	21.4	19.2	22.0
4	21.1	23.5	22	24.1	21.2	23.7	21.8	24.1

Table 5.1.1 Average Lesion Size at the Time of Detection

5.2 Histogram of Lesion Size at the Time of Detection

A distribution of lesion size at the time of detection was also of interest. Figures 5.2.1 and 5.2.2 show histograms of lesion size at the time of detection with CT, mammography, and BSE for the different screening regimes. Because the difference between screening ages 40 to 80 and 40 to 125 or 50 to 80 and 50 to 125 was slight, screening from age 40 to 80 and screening from age 50 to 80 are shown for the 4 screening intervals explored. Figures 5.2.3 and 5.2.4 illustrating the histograms for screening starting at age 40 to end of life and starting at age 50 to end of life can be found in Appendix A. As expected from the sensitivity data, the tumors were detected at smaller sizes with CT compared to Mammography. No screening (BSE) had the least efficiency and led to detection at larger sizes. As illustrated, lesion sizes at detection are concentrated at higher sizes with BSE, spread out with mammography, and most concentrated at lower sizes with CT. Longer screening interval leads to larger tumor sizes at detection.

Screening starting at age 50 instead of 40 negatively impacts tumor size at detection. As mentioned earlier in the growth model, breast tumors approach 30 mm diameters with time. This explains the relatively significant population whose cancer gets detected at 30 mm diameter. Because breast cancer growth rates are higher at younger ages tumors of most people who contract breast cancer at younger ages reach 30 mm before screening starts which leads to a detection lesion size of 30 mm for most of this population which also explains why screening starting at a later age results in a higher fraction of people having their tumors detected at 30 mm.

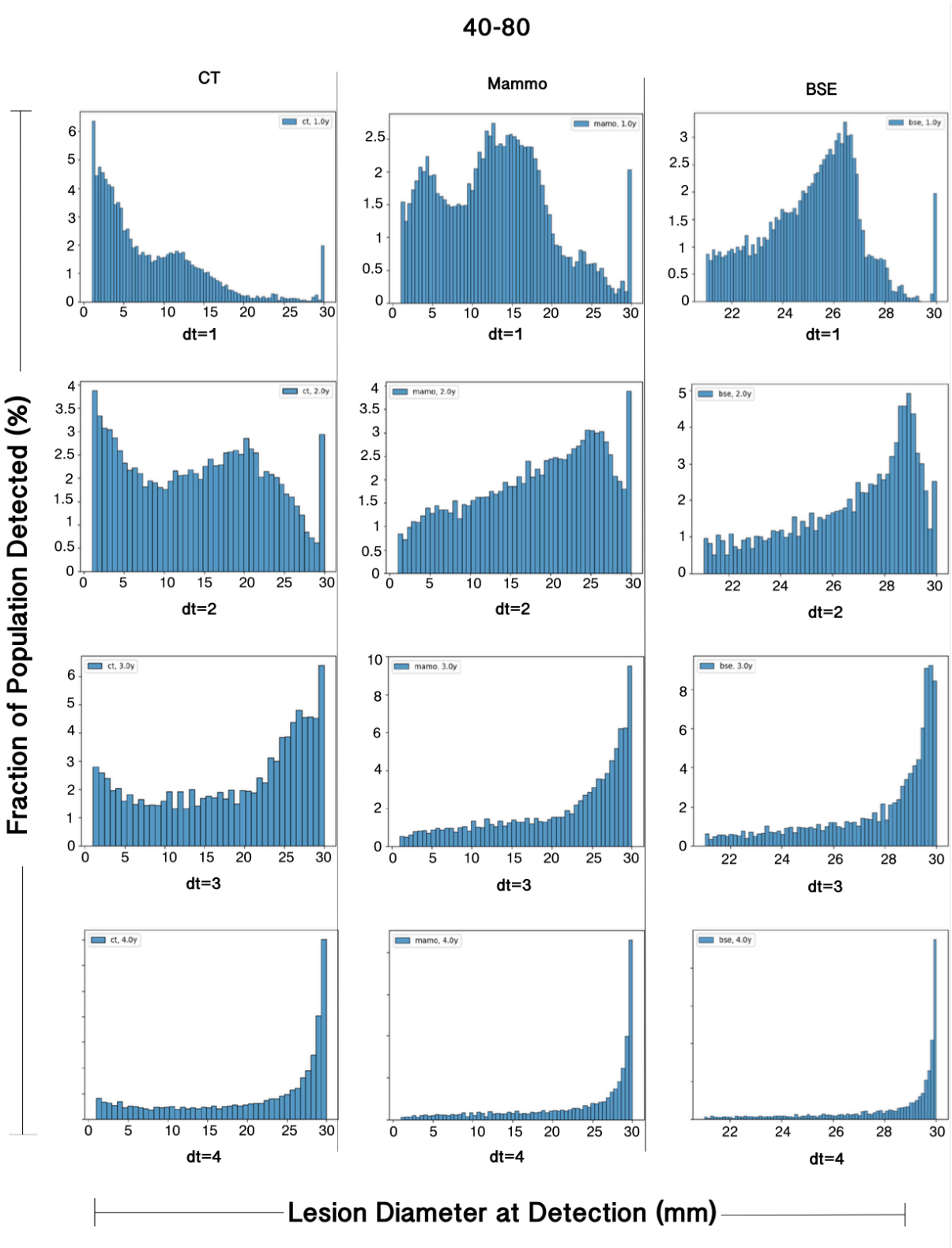

Fig 5.2.1 Histogram of Lesion Size at Time of Detection for Screening Starting at Age 40 Until Age 80

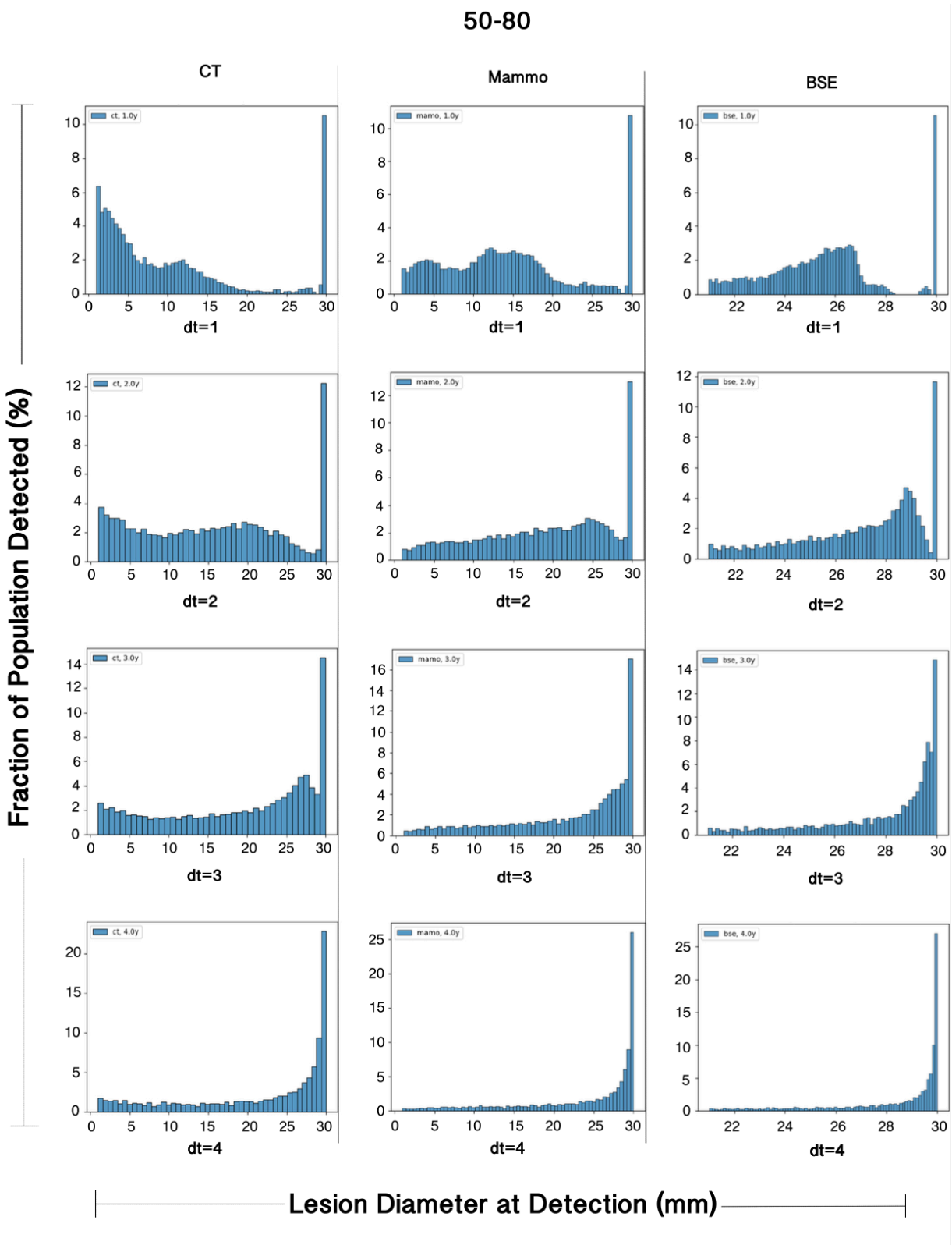

Fig 5.2.2 Histogram of Lesion Size at Time of Detection for Screening Starting at Age 50 and Ending at Age 80

5.3 Years of life saved

Years of life saved shows the number of years the woman lives longer than she would if she does not go through screening. It is calculated by subtracting the age of death with no screening (BSE) from the age of death with screening which varies depending on the screening regime and modality. This parameter is an indication of how many years of the woman's life are saved thanks to early detection because of the screening performed.

Figure 5.3.1 (a,b,c,d) illustrates the average years of life saved by screening interval for both CT and mammography in all regimes for the total population. As expected, years of life saved is higher for CT than for mammography. It also increases with higher screening frequency or lower screening intervals which means the benefit of screening is higher with higher screening frequency. As mentioned in section 5.1, higher screening frequency leads to detection at lower sizes which results in a better prognosis and explains this result. Additionally, since the difference between the sensitivities of CT and mammography is higher at lower sizes, we expected the difference in years of life saved between the two modalities to be higher with higher screening frequency. The plots shown in the figure confirm this and indicate that the benefit of screening with CT is higher at higher screening frequency.

For the total population, screening at 1-year intervals starting at age 40 until age 80 results in the average years of life saved of 3.4 years for CT and 2.3 years for mammography. Averaged over all regimes, years of life saved with CT were 0.5 year higher than with mammography and the difference was more significant at higher frequencies. The highest years of life saved was for the yearly screening of 40- to 80-year-olds with CT while the lowest was for screening starting at age 50 to end of life at 5 years interval. Screening until the end of life instead of age 80 slightly lowered the years of life saved. This can be explained by the fact that the remaining life span is longer at younger ages.

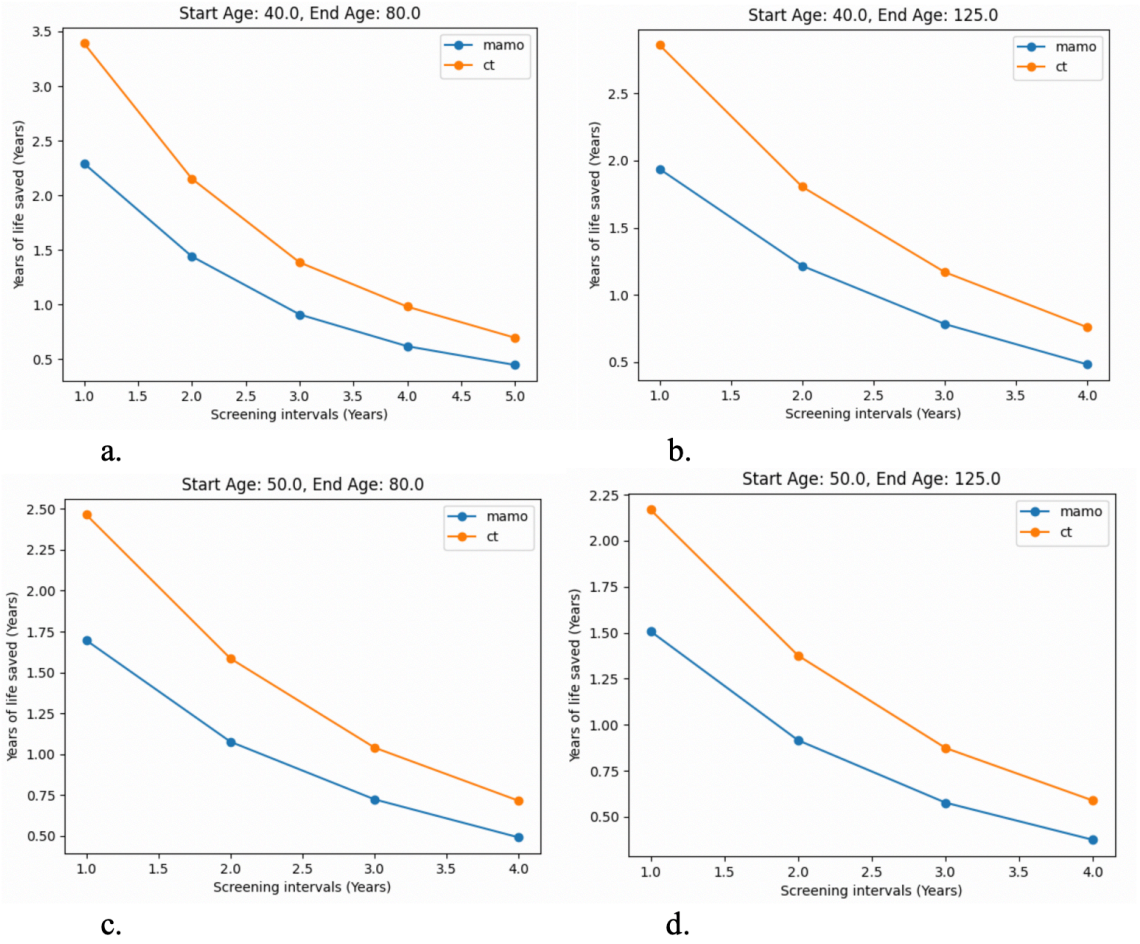

Fig 5.3.1 Average Years of Life Saved by Screening Interval for 4 Screening Regimes for Total

Figure 5.3.2 (a,b,c,d) shows the average years of life saved by screening interval for both CT and mammography in all regimes for different races. As seen in the plots, years of life saved is significantly higher for Asian women compared to the other races, and there are slight differences among the other races. It should be noted that the population of Asians and American Indians is much lower than the other races. This leads to higher variance in the results of multiple simulations for these two races thus the results for Asians and American Indians are statistically less reliable.

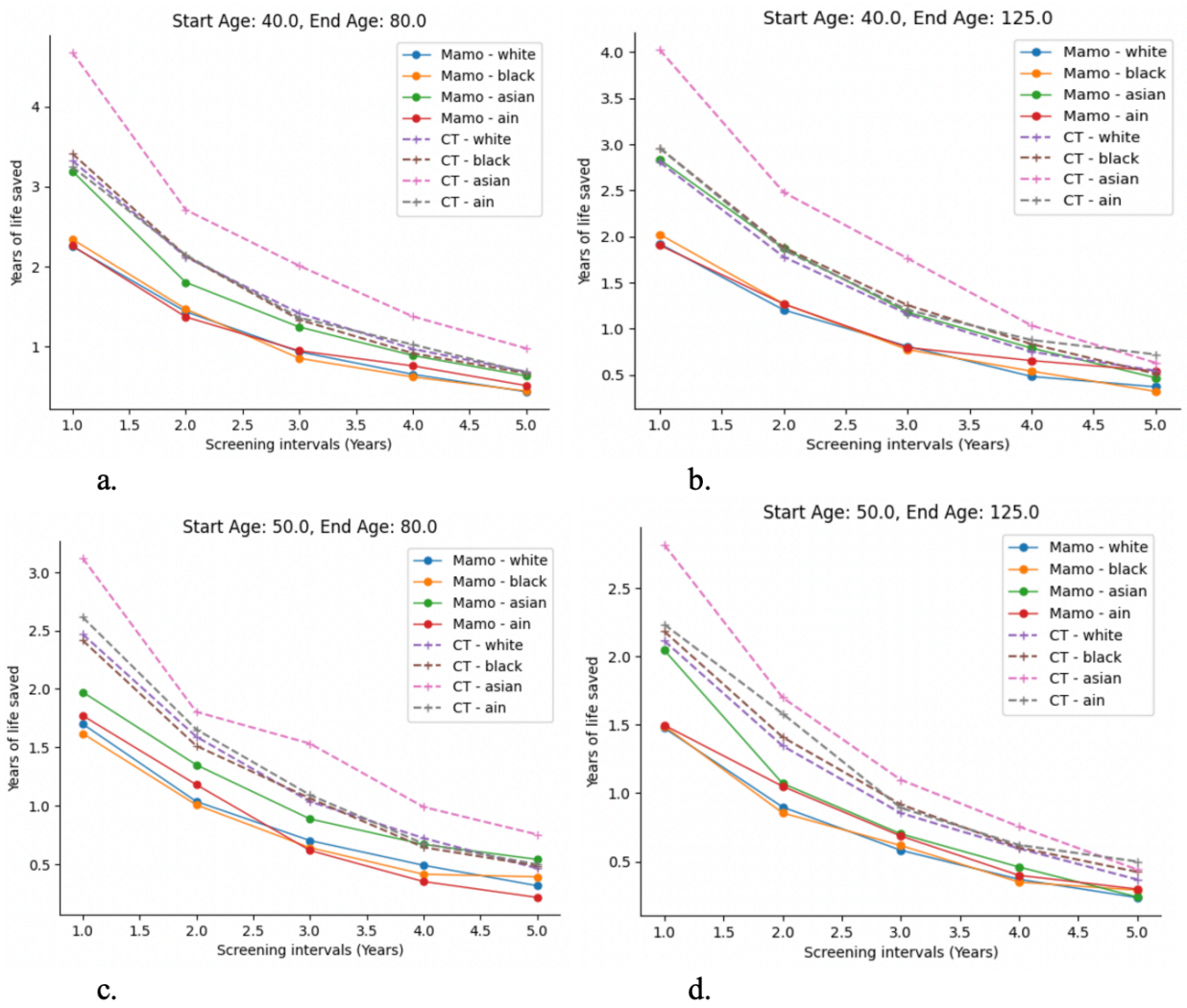

Fig 5.3.2 Average Years of Life Saved by Screening Interval for 4 Screening Regimes for the Different Races

5.4 Years of Life Saved as a Function of Age at the Time of Breast Cancer Detection

Figure 5.4.1 (a,b,c,d) illustrates years of life saved as a function of age at breast cancer detection. As can be seen, years of life saved is higher with CT than with Mammography. Except for the few points at the youngest ages, the overall trend shows higher years of life saved for younger ages of detection which means that screening benefits younger women who get breast cancer more than older women.

As can be seen, years of life saved first increases, reaches a peak, and then decreases as detection age increases. For screening starting at age 40 the years of life saved peaks at around detection age between 40 and 45 years old and for screening starting at age 50 it peaks between 50 and 55 years old. The population whose cancer gets detected at around the screening start age is the accumulation of the people who have contracted breast cancer

between the age 15 and the screening start age. Because cancer growth rates are much higher at younger ages, the relatively longer time elapsed between cancer incidence and detection leads to higher tumor sizes at detection which in turn leads to a worse prognosis. As we move forward from the screening start age the proportion of this group compared to the total population decreases and has less and less influence on years of life saved. This explains the lower years of life saved at the beginning of the plots.

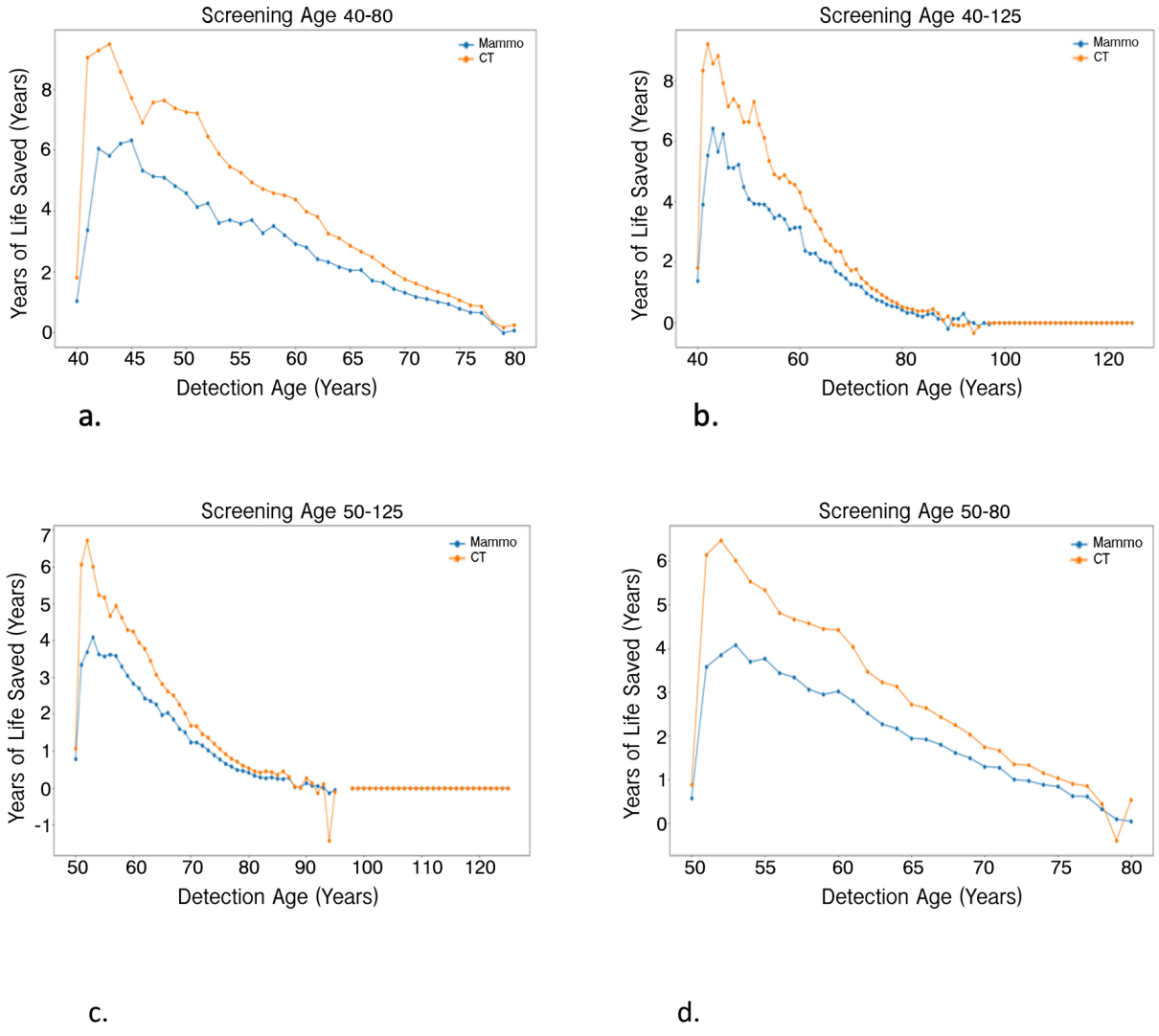

Fig 5.4.1 Years of Life Saved by Age of Breast Cancer Detection

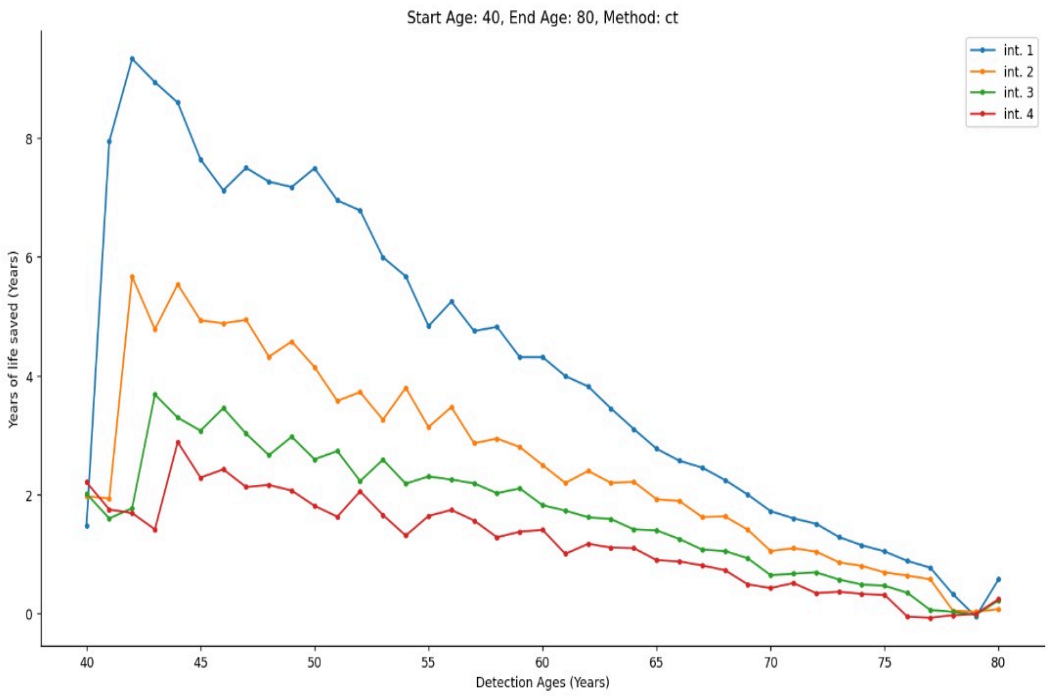

Fig 5.4.2 Years of Life Saved by Age of Breast Cancer Detection

Fig 5.4.2 illustrates years of life saved as a function of age at breast cancer detection for different screening intervals. Shorter screening intervals benefit younger women more as the tumor growth rate is higher at younger ages. As we approach older ages screening interval has less effect on years of life saved. This suggests that lower screening frequency may be appropriate at older ages.

5.5 Years of Life Saved per the Number of Tests Performed

Years of life saved per number of tests performed was also calculated and compared as an indicator of screening efficacy. Because a lower screening interval means higher screening frequency and therefore earlier detection while a higher number of tests are performed, we expected there to be a peak performance point indicated by this parameter. Figure 5.4.1. (a, b, c, d) show years of life saved per number of tests performed by screening intervals for all races combined for each screening regime. As illustrated in the figures, years of life saved per the number of screenings performed is highest for screening from age 50 to 80 for screening with both CT and mammography. On average the results are better for CT than for mammography by approximately 50%. These figures also indicate that the screening interval of 2 years is optimum and leads to higher efficiency. Based on these results we concluded that screening every 2 years starting at age 50 until age 80 with CT is the most efficient screening protocol for all races combined.

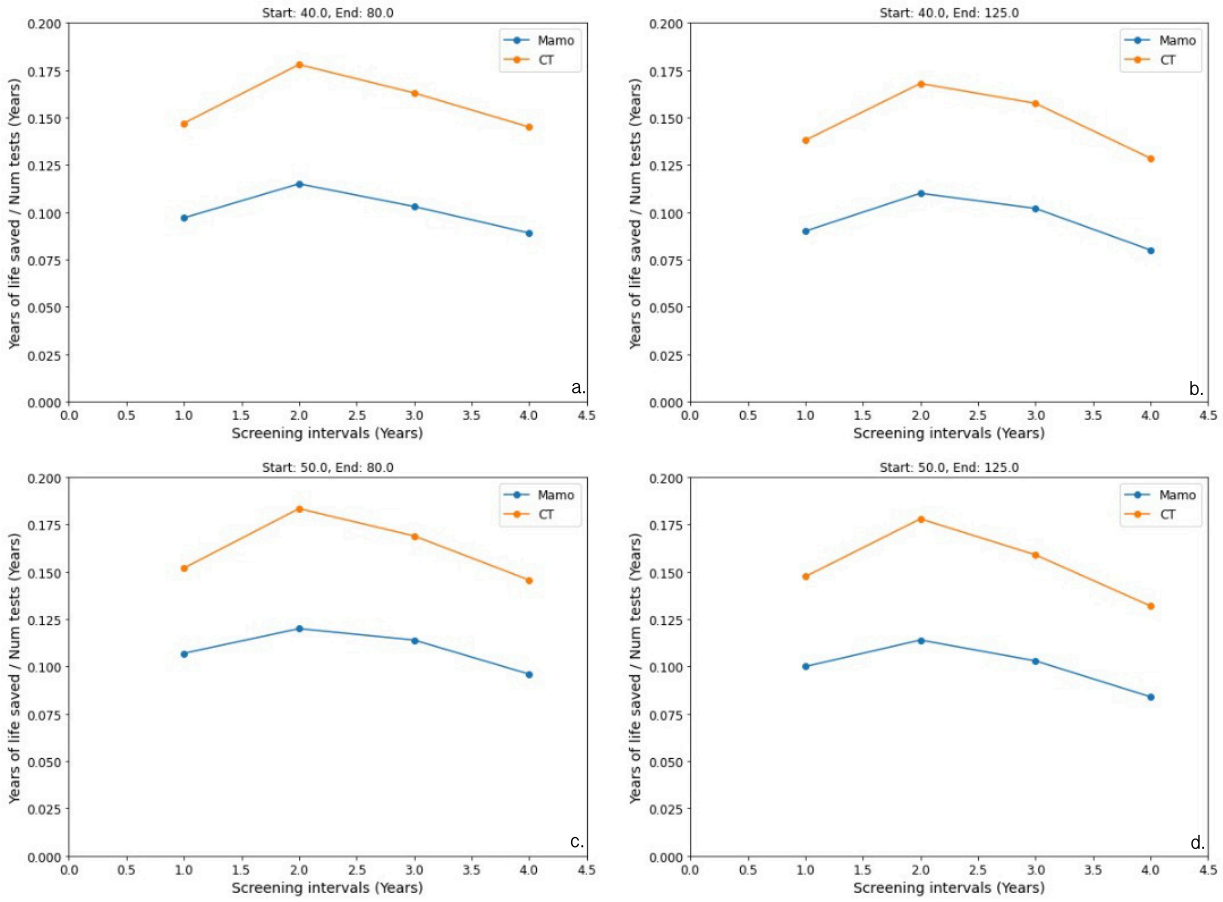

Fig 5.5.1. (a, b, c, d) Years of Life Saved for All Races per Number of Tests Performed

Years of life saved per the number of tests performed is shown in fig 5.5.2. (a, b, c, d) for different races. As illustrated, the results are better for CT than mammography for each race and significantly better for Asians than other races with both modalities. Screening from age 50 to 80 every 2 years has the best results for White women, screening every 3 years starting at age 50 until 80 has the best results for Asians, and screening every 2 years starting at age 50 to the end of life is best for Black or African Americans, and American Indians and Alaska Natives. It should be noted that because the population of Asians and American Indians and Alaska natives are significantly lower the results for these two groups has higher variance and are not reliable.

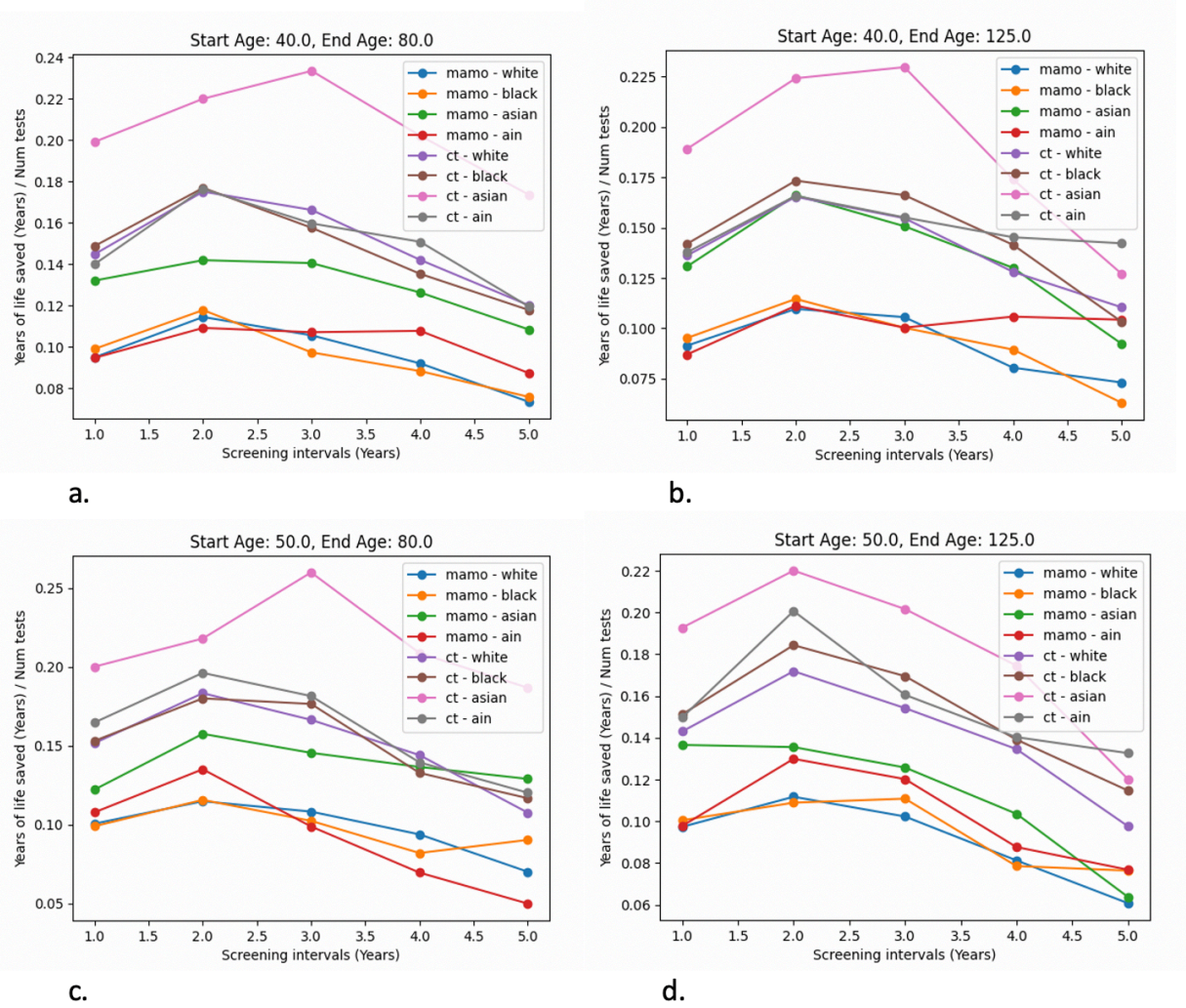

Fig 5.5.2. a, b, c, d Years of Life Saved per Number of Tests for Different Races

In conclusion, while screening with CT starting at age 50 until 80 at 2-year intervals results in the highest years of life saved per number of tests for the total population (all races combined), different screening programs lead to better results for each race and should be considered for screening policy decisions.

A limitation of the project is that it considers solid tumor size as the only diagnostic criterion for breast cancer. While crucial in determining the status of many breast cancers, solid tumor size is not sufficient to diagnose all breast cancers. Some types of breast cancer do not necessarily appear as masses or lumps. Microcalcification, lobular breast cancer, and IBC are examples of such breast cancers. While microcalcifications are mainly detected on mammograms, their shape and distribution are important indicators of breast cancer in addition to their size [64]. Furthermore, lobular breast cancer is difficult to detect with mammography due to its diffusive growth pattern. Ultrasound and more so MRI have proven to have higher sensitivity rates to detect this type of cancer [65-67]. Considering additional

determining factors of breast cancer and incorporating data from diagnostic tools other than mammography and CT such as MRI and Ultrasound can make for more comprehensive future studies.

Adipose/glandular tissue fraction affects breast cancer detection in images [68] [69] . Since glandular tissue appears white on a mammogram it can obscure breast cancers. Thus, a higher fraction of glandular tissue makes breast cancer detection more difficult and can result in missed cancers [69, 70]. This variable was not considered in this project and can be implemented as another parameter in future work for more accurate results.

Radiation-induced breast cancer may result from exposure to ionizing radiation and depends on the radiation dose. While factors such as imaging equipment and parameters, and breast size and density affect average glandular radiation dose [71, 72], a study has found average glandular radiation dose (AVG) with a mean of 6.5 mGy for mammography and 8.2 mGy for CT.[73] Differences in radiation dose of mammography and breast CT, and radiation-induced breast cancers were not considered in this study and can be an area to explore in future research.

One of the challenges facing this research is the fact that breast CT is a relatively new technology and is not yet clinically available for screening. While studies are being conducted on breast CT, one of the limitations that this fact imposes is that there is limited data available for it compared to mammography, and more research on this technology is needed. As our findings suggest, breast CT is more efficient than mammography in terms of years of life saved per number of tests performed. We hope that this study will contribute to addressing the potential of breast CT to be embraced clinically.

Breast tomosynthesis has the potential to serve as a substitute for mammography [74] and can be another modality incorporated in future studies to compare with mammography and breast CT both on its own and in conjunction with mammography. Tomosynthesis has higher sensitivity and specificity rates compared to mammography and there is a lower probability of breast cancer being missed due to overlapping tissue with this technology [75]. It has better detectability, particularly in patients with high breast density [76].

Using available data of breast tomosynthesis sensitivity rates as a function of lesion size, the probability of breast cancer detection can be calculated for tomosynthesis and used in future analysis as was done for CT and mammography in this project.

6. Appendix

Appendix A:

Histogram of tumor size at the time of detection for screening starting at age 40 to end of life and screening from age 50 to end of life are shown in this section.

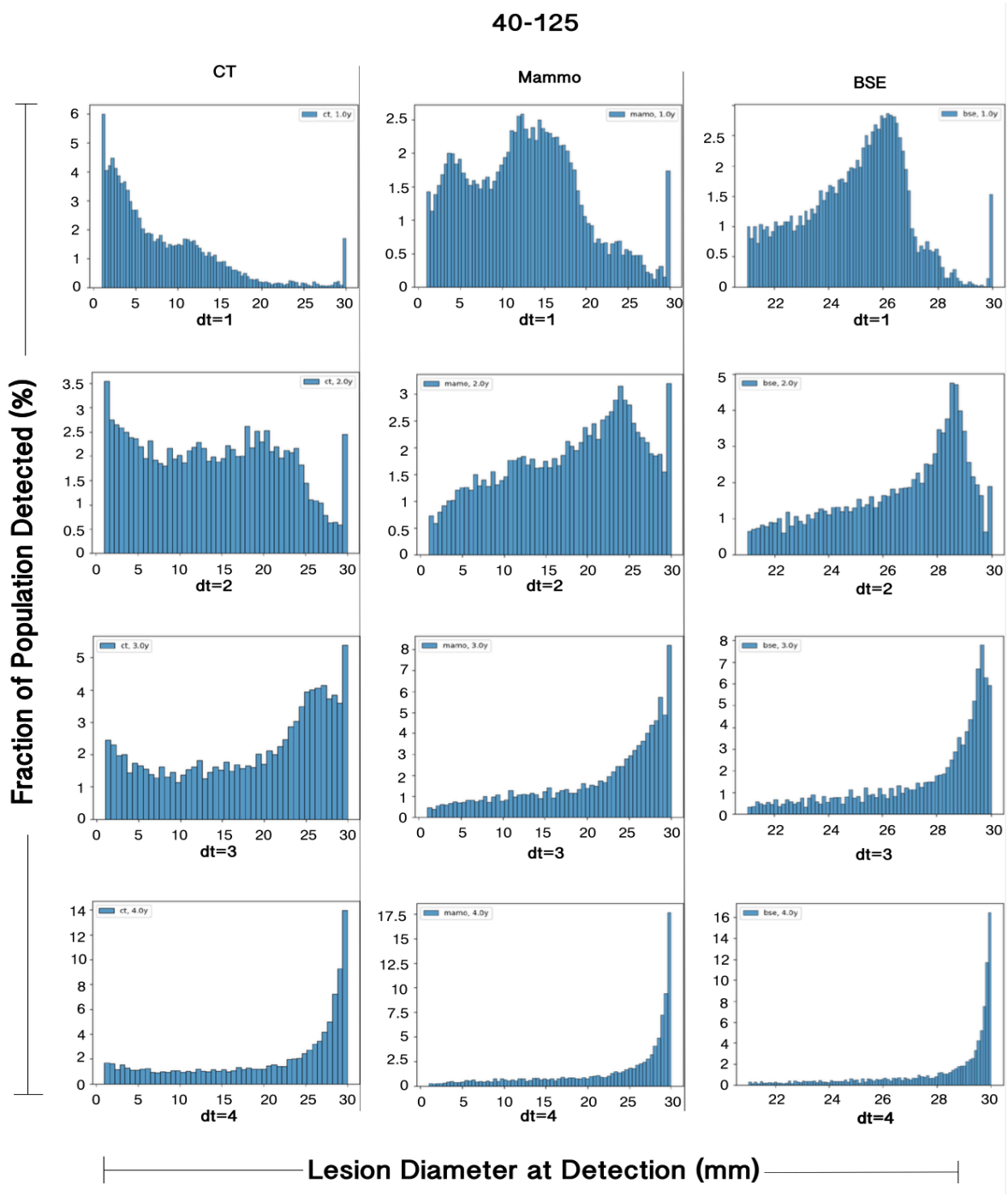

Fig 5.2.3 Histogram of Lesion Size at Time of Detection for Screening 40 – End of Life

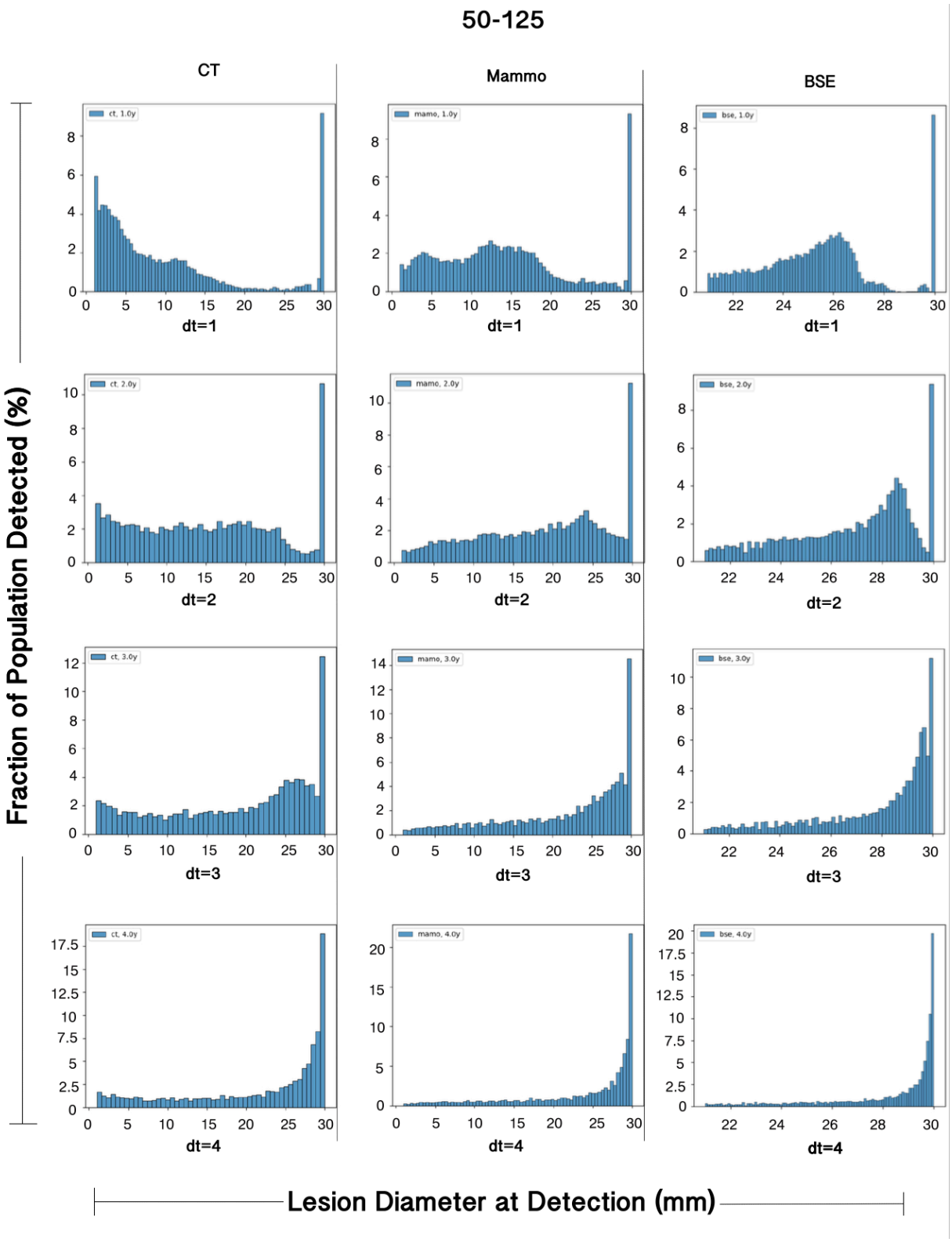

Fig 5.2.4 Histogram of Lesion Size at Time of Detection for Screening 50 – End of Life

References:

1. Therese B. Bevers MD, B.O.A.M., Ermelinda Bonaccio MD, Sandra Buys MD, Mary B. Daly MD, PhD, Peter J. Dempsey MD, William B. Farrar MD, Irving Fleming MD, Judy E. Garber MD, MPH, Randall E. Harris MD, PhD, Alexandra S. Heerdt MD, Mark Helvie MD, John G. Huff MD, Nazanin Khakpour MD, Seema A. Khan MD, Helen Krontiras MD, Gary Lyman MD, MPH, Elizabeth Rafferty MD, Sara Shaw MD, Mary Lou Smith JD, MBA, Theodore N. Tsangaris MD, Cheryl Williams MD, and Thomas Yankeelov PhD. *Breast Cancer Screening and Diagnosis*. 2009; Available from: https://jnccn.org/view/journals/jnccn/7/10/article-p1060.xml#R1

.
2. *Breast Cancer Facts and Figures 2007-2008*. Available from: http://www.cancer.org/downloads/STT/BCFF-Final.pdf.
3. Society, A.C. *Breast Cancer Facts and Figures*. 2016; Available from: https://www.cancer.org/content/dam/cancer-org/research/cancer-facts-and-statistics/breast-cancer-facts-and-figures/breast-cancer-facts-and-figures-2017-2018.pdf.
4. Miller, K.D., et al., *Cancer treatment and survivorship statistics, 2016.* CA Cancer J Clin, 2016. **66**(4): p. 271-89.
5. Alkabban, F.M. and T. Ferguson, *Breast Cancer*, in *StatPearls*. 2022, StatPearls Publishing

Copyright © 2022, StatPearls Publishing LLC.: Treasure Island (FL).
6. Society, A.C. *Cancer Facts and Figures*. Available from: https://www.cancer.org/research/cancer-facts-statistics.html.
7. Society, A.C. *Breast Cancer Facts & Figures*. Available from: https://www.cancer.org/research/cancer-facts-statistics/breast-cancer-facts-figures.html.
8. Howlader N, N.A., Krapcho M, et al., *SEER Cancer Statistics Review (CSR) 1975-2014.*
9. NIH, N.C.I., Surveillance, Epidemiology and End Results Program. *Recent Trends in SEER Age-Adjusted Incidence Rates, 2000-2019*. Available from: https://seer.cancer.gov/statistics-network/explorer/application.html?site=1&data_type=1&graph_type=2&compareBy=sex&chk_sex_3=3&chk_sex_2=2&rate_type=2&race=1&age_range=1&hdn_stage=101&advopt_precision=1&advopt_show_ci=on&hdn_view=0&advopt_display=2.
10. NIH, N.C.I., Surveillance, Epidemiology and End Results Program. *Breast Recent Trends in SEER Age-Adjusted Incidence Rates, 2000-2019*. Available from: https://seer.cancer.gov/statistics-network/explorer/application.html?site=55&data_type=1&graph_type=2&compareBy=race&chk_race_1=1&chk_race_5=5&chk_race_4=4&chk_race_3=3&chk_race_2=2&rate_type=2&sex=3&age_range=1&stage=101&advopt_precision=4&advopt_show_ci=on&hdn_view=0&advopt_display=2.
11. Niell, B.L., et al., *Screening for Breast Cancer.* Radiol Clin North Am, 2017. **55**(6): p. 1145-1162.
12. Smith, R.A., et al., *The randomized trials of breast cancer screening: what have we learned?* Radiol Clin North Am, 2004. **42**(5): p. 793-806, v.

13. Tabár, L., et al., *Insights from the breast cancer screening trials: how screening affects the natural history of breast cancer and implications for evaluating service screening programs.* Breast J, 2015. **21**(1): p. 13-20.
14. Oeffinger, K.C., et al., *Breast Cancer Screening for Women at Average Risk: 2015 Guideline Update From the American Cancer Society.* Jama, 2015. **314**(15): p. 1599-614.
15. Bjurstam, N., et al., *The Gothenburg Breast Cancer Screening Trial: preliminary results on breast cancer mortality for women aged 39-49.* J Natl Cancer Inst Monogr, 1997(22): p. 53-5.
16. Bjurstam, N., et al., *The Gothenburg Breast Screening Trial.* Cancer, 2003. **97**(10): p. 2387-96.
17. Institute of, M. and C. National Research Council Committee on the Early Detection of Breast, in *Mammography and Beyond: Developing Technologies for the Early Detection of Breast Cancer: A Non-Technical Summary*, M. Patlak, et al., Editors. 2001, National Academies Press (US)
Copyright 2001 by the National Academy of Sciences. All rights reserved.: Washington (DC).
18. Force, U.P.S.T. *Breast Cancr: Screening, Final Recommendation*. 2016; Available from: https://www.uspreventiveservicestaskforce.org/uspstf/recommendation/breast-cancer-screening.
19. Siu, A.L., *Screening for Breast Cancer: U.S. Preventive Services Task Force Recommendation Statement.* Ann Intern Med, 2016. **164**(4): p. 279-96.
20. *Screening for breast cancer: U.S. Preventive Services Task Force recommendation statement.* Ann Intern Med, 2009. **151**(10): p. 716-26, w-236.
21. Monticciolo, D.L., et al., *Breast Cancer Screening for Average-Risk Women: Recommendations From the ACR Commission on Breast Imaging.* J Am Coll Radiol, 2017. **14**(9): p. 1137-1143.
22. Monticciolo, D.L., et al., *Breast Cancer Screening in Women at Higher-Than-Average Risk: Recommendations From the ACR.* J Am Coll Radiol, 2018. **15**(3 Pt A): p. 408-414.
23. Robertson, F.M., et al., *Inflammatory Breast Cancer: The Disease, the Biology, the Treatment.* CA: A Cancer Journal for Clinicians, 2010. **60**(6): p. 351-375.
24. D.J.P. van Uden, H.W.M.v.L., A.H. Westenberg, J.H.W. de Wilt, C.F.J.M. Blanken-Peeters,, *Inflammatory breast cancer: An overview.* Critical Reviews in Oncology/Hematology,
, 2015. **Volume 93**(Issue 2): p. 116-126.
25. Gentle, J.E., *Random Number Generation and Monte Carlo Methods.* Statistics and Computing 1998.
26. Jokar, E. and M. Mikaili, *Assessment of human random number generation for biometric verification.* J Med Signals Sens, 2012. **2**(2): p. 82-7.
27. Figurska, M., M. Stańczyk, and K. Kulesza, *Humans cannot consciously generate random numbers sequences: Polemic study.* Med Hypotheses, 2008. **70**(1): p. 182-5.
28. L'Ecuyer, P., *Random Number Generation*, in *Handbook of Computational Statistics: Concepts and Methods*, J.E. Gentle, W.K. Härdle, and Y. Mori, Editors. 2012, Springer Berlin Heidelberg: Berlin, Heidelberg. p. 35-71.
29. Edmonds, A.R., *The Generation of Pseudo-Random Numbers on Electronic Digital Computers.* The Computer Journal, 1960. **2**(4): p. 181-185.

30. Numbers, G.P. 2022; Available from: https://www.mathworks.com/help/stats/generating-random-data.html.
31. *Quantitative Data Analysis: Microsimulation*. Available from: https://www.urban.org/research/data-methods/data-analysis/quantitative-data-analysis/microsimulation.
32. Citro, C.H., EA., editors., *Review and Recommendations. Vol. Vol I. National Research Council; 1991. Improving Information for Social Policy Decisions: The Uses of Microsimulation Modeling.*
33. Rutter, C.M., A.M. Zaslavsky, and E.J. Feuer, *Dynamic microsimulation models for health outcomes: a review.* Med Decis Making, 2011. **31**(1): p. 10-8.
34. *International Microsimulation Association.*
35. Habbema, J.D., et al., *The MISCAN simulation program for the evaluation of screening for disease.* Comput Methods Programs Biomed, 1985. **20**(1): p. 79-93.
36. Habbema, J.D., et al., *Model building on the basis of Dutch cervical cancer screening data.* Maturitas, 1985. **7**(1): p. 11-20.
37. van Oortmarssen, G.J., et al., *A model for breast cancer screening.* Cancer, 1990. **66**(7): p. 1601-12.
38. Loeve, F., et al., *The MISCAN-COLON simulation model for the evaluation of colorectal cancer screening.* Comput Biomed Res, 1999. **32**(1): p. 13-33.
39. Draisma, G., et al., *Lead times and overdetection due to prostate-specific antigen screening: estimates from the European Randomized Study of Screening for Prostate Cancer.* J Natl Cancer Inst, 2003. **95**(12): p. 868-78.
40. Longini, I.M., Jr., et al., *Containing a large bioterrorist smallpox attack: a computer simulation approach.* Int J Infect Dis, 2007. **11**(2): p. 98-108.
41. Ackerman, E., et al., *Simulation of mechanisms of viral interference in influenza.* Int J Epidemiol, 1990. **19**(2): p. 444-54.
42. Ackerman, E., et al., *Simulation of stochastic micropopulation models--I. The SUMMERS simulation shell.* Comput Biol Med, 1993. **23**(3): p. 177-98.
43. Peterson, D., et al., *Simulation of stochastic micropopulation models--II. VESPERS: epidemiological model implementations for spread of viral infections.* Comput Biol Med, 1993. **23**(3): p. 199-213.
44. Cassels, S., S.J. Clark, and M. Morris, *Mathematical models for HIV transmission dynamics: tools for social and behavioral science research.* J Acquir Immune Defic Syndr, 2008. **47 Suppl 1**(Suppl 1): p. S34-9.
45. Castiglione, F., et al., *Optimization of HAART with genetic algorithms and agent-based models of HIV infection.* Bioinformatics, 2007. **23**(24): p. 3350-5.
46. Vogelaar, I., et al., *How much can current interventions reduce colorectal cancer mortality in the U.S.? Mortality projections for scenarios of risk-factor modification, screening, and treatment.* Cancer, 2006. **107**(7): p. 1624-33.
47. (CISNET), N.C.I.C.I.a.S.M.N., *Colorectal Cancer Mortality Projections. Modeling the impact of cancer control efforts on US colorectal cancer mortality Dec. 2007* 2008.
48. Yong, J.H.E., et al., *The OncoSim-Breast Cancer Microsimulation Model.* Curr Oncol, 2022. **29**(3): p. 1619-1633.
49. *US Population by Age and Race*. 2016 [cited 2017 Aug]; Available from: https://factfinder.census.gov/faces/tableservices/jsf/pages/productview.xhtml?pid=PEP_2016_PEPALL5N&prodType=table.

50. *US All Races Combined Population by Age and Race*. 2016 [cited 2019 March]; Available from: https://factfinder.census.gov/faces/tableservices/jsf/pages/productview.xhtml?pid=PEP_2016_PEPAGESEX&prodType=table.
51. *US Female Death Rates from All Causes*. 2014; Available from: https://www.cdc.gov/nchs/data/nvsr/nvsr65/nvsr65_04.pdf).
52. *US Breast Cancer Death Rates by Age*. Available from: https://seer.cancer.gov/explorer/application.php?site=55&data_type=2&stat_type=3&compareBy=race&chk_sex_3=3&chk_race_1=1&chk_race_5=5&chk_race_4=4&chk_race_3=3&chk_race_2=2&advopt_precision=4&advopt_show_se=on&advopt_show_ci=on&showDataFor=sex_3.
53. *Breast Cancer Incidence Rates*. Available from: https://seer.cancer.gov/explorer/application.html?site=55&data_type=1&graph_type=2&compareBy=race&chk_race_1=1&chk_race_5=5&chk_race_4=4&chk_race_3=3&chk_race_2=2&sex=3&age_range=1&stage=101&rate_type=2&advopt_precision=4&advopt_show_ci=on&advopt_display=2.
54. Spratt, J.S., R.A. Greenberg, and L.S. Heuser, *Geometry, growth rates, and duration of cancer and carcinoma in situ of the breast before detection by screening.* Cancer Research, 1986. **46**(2): p. 970-974.
55. Förnvik, D., et al., *Breast tomosynthesis: accuracy of tumor measurement compared with digital mammography and ultrasonography.* Acta radiologica, 2010. **51**(3): p. 240-247.
56. Dahan, M., et al., *Has tumor doubling time in breast cancer changed over the past 80 years? A systematic review.* Cancer Med, 2021. **10**(15): p. 5203-5217.
57. Michaelson, J., et al., *Estimates of breast cancer growth rate and sojourn time from screening database information.* Journal of Womens Imaging, 2003. **5**: p. 11-19.
58. Peer, P.G., et al., *Age-dependent growth rate of primary breast cancer.* Cancer, 1993. **71**(11): p. 3547-51.
59. Chen, L., et al., *Simulated lesion, human observer performance comparison between thin-section dedicated breast CT images versus computed thick-section simulated projection images of the breast.* Physics in Medicine and Biology, 2015. **60**(8): p. 3347-3358.
60. Schwab, F.D., et al., *Self-detection and clinical breast examination: comparison of the two "classical" physical examination methods for the diagnosis of breast cancer.* Breast, 2015. **24**(1): p. 90-2.
61. Güth, U., et al., *Tumor size and detection in breast cancer: Self-examination and clinical breast examination are at their limit.* Cancer Detect Prev, 2008. **32**(3): p. 224-8.
62. Shaevitch, D., et al., *Tumor size distribution of invasive breast cancers and the sensitivity of screening methods in the Canadian National Breast Screening Study.* Journal of Cancer Research and Therapeutics, 2017. **13**(3): p. 562-569.
63. Michaelson, J.S., et al., *Predicting the survival of patients with breast carcinoma using tumor size.* Cancer: Interdisciplinary International Journal of the American Cancer Society, 2002. **95**(4): p. 713-723.
64. Anderson, M.E., et al., *The detection of breast microcalcifications with medical ultrasound.* J Acoust Soc Am, 1997. **101**(1): p. 29-39.

65. Wilson, N., et al., *Lobular Breast Cancer: A Review.* Frontiers in Oncology, 2021. **10**.
66. Koufopoulos N, P.I., Gouloumis AR, Ieronimaki AI, Zacharatou A, Spathis A, Leventakou D, Economopoulou P, Psyrri A, Arkadopoulos N, Panayiotides IG, *Diagnostically Challenging Subtypes of Invasive Lobular Carcinomas: How to Avoid Potential Diagnostic Pitfalls.* Diagnostics, 2022. **12**.
67. Hilleren, D.J., et al., *Invasive lobular carcinoma: mammographic findings in a 10-year experience.* Radiology, 1991. **178**(1): p. 149-54.
68. Nelson, T.R., et al., *Classification of breast computed tomography data.* Med Phys, 2008. **35**(3): p. 1078-86.
69. Berg, W.A., et al., *Screening Algorithms in Dense Breasts: AJR Expert Panel Narrative Review.* AJR Am J Roentgenol, 2021. **216**(2): p. 275-294.
70. Soguel, L., et al., *Adiposity, breast density, and breast cancer risk: epidemiological and biological considerations.* Eur J Cancer Prev, 2017. **26**(6): p. 511-520.
71. Boone, J.M., et al., *Dedicated breast CT: radiation dose and image quality evaluation.* Radiology, 2001. **221**(3): p. 657-67.
72. Olgar, T., T. Kahn, and D. Gosch, *Average glandular dose in digital mammography and breast tomosynthesis.* Rofo, 2012. **184**(10): p. 911-8.
73. O'Connell, A., et al., *Cone-beam CT for breast imaging: Radiation dose, breast coverage, and image quality.* AJR Am J Roentgenol, 2010. **195**(2): p. 496-509.
74. Sechopoulos, I., *A review of breast tomosynthesis. Part I. The image acquisition process.* Medical Physics, 2013. **40**(1): p. 014301.
75. Whelehan, P., et al., *Digital breast tomosynthesis: sensitivity for cancer in younger symptomatic women.* Br J Radiol, 2021. **94**(1119): p. 20201105.
76. Park, J.M., et al., *Breast tomosynthesis: present considerations and future applications.* Radiographics, 2007. **27 Suppl 1**: p. S231-40.